1977

The use of DMSP and SMS-2 digital satellite data for identifying marine fog in the eastern North Pacific Ocean area.

Ihli, Carl Bolton, Jr.

NAVAL POSTGRADUATE SCHOOL
Monterey, California

THESIS

THE USE OF DMSP AND SMS-2 DIGITAL SATELLITE DATA FOR IDENTIFYING MARINE FOG IN THE EASTERN NORTH PACIFIC OCEAN AREA

by

Carl Bolton Ihli, Jr.

March 1977

Thesis Advisor: R. J. Renard

SECURITY CLASSIFICATION OF THIS PAGE (When Data Entered)

REPORT DOCUMENTATION PAGE

READ INSTRUCTIONS BEFORE COMPLETING FORM

1. REPORT NUMBER: NPS-63Ih77031
2. GOVT ACCESSION NO.:
3. RECIPIENT'S CATALOG NUMBER:

4. TITLE (and Subtitle): The Use of DMSP and SMS-2 Digital Satellite Data for Identifying Marine Fog in the Eastern North Pacific Ocean Area

5. TYPE OF REPORT & PERIOD COVERED: Master's Thesis; March 1977

6. PERFORMING ORG. REPORT NUMBER:

7. AUTHOR(s): Carl B. Ihli, Jr.
In conjunction with
Robert J. Renard

8. CONTRACT OR GRANT NUMBER(s):

9. PERFORMING ORGANIZATION NAME AND ADDRESS: Naval Postgraduate School
Monterey, California 93940

10. PROGRAM ELEMENT, PROJECT, TASK AREA & WORK UNIT NUMBERS: 62759N; ZF5255; ZF52551713;NPSOM-1

11. CONTROLLING OFFICE NAME AND ADDRESS: Naval Air Systems Command, 370C
Washington, D. C. 20360

12. REPORT DATE: March 1977

13. NUMBER OF PAGES: 99

14. MONITORING AGENCY NAME & ADDRESS(if different from Controlling Office): Naval Postgraduate School
Monterey, California 93940

15. SECURITY CLASS. (of this report): Unclassified

15a. DECLASSIFICATION/DOWNGRADING SCHEDULE:

16. DISTRIBUTION STATEMENT (of this Report): Approved for public release; distribution unlimited.

17. DISTRIBUTION STATEMENT (of the abstract entered in Block 20, if different from Report):

18. SUPPLEMENTARY NOTES:

19. KEY WORDS (Continue on reverse side if necessary and identify by block number): fog; marine fog; weather satellite; North Pacific Ocean; ocean fog; DMSP satellite data; SMS-2 satellite data; geosynchronous satellite; meteorological satellite; marine visibility.

20. ABSTRACT (Continue on reverse side if necessary and identify by block number):

Defense Meteorological Satellite Program (DMSP) and Synchronous Meteorological Satellite (SMS-2) digital satellite data, both visual and infrared, are processed and analyzed in context with transient/stationary synoptic ship reports, in an effort to identify areas of marine fog occurrence. The eastern North Pacific Ocean was chosen as the

DD FORM 1 JAN 73 1473 EDITION OF 1 NOV 65 IS OBSOLETE
S/N 0102-014-6601 |

SECURITY CLASSIFICATION OF THIS PAGE (When Data Entered)

area of study; for various reasons the period was limited to 5-9 August 1976. Histograms and two-dimensional plots of visual and infrared data are generated as a function of five categories of fog/no-fog occurrence. Optimal ranges of visual and infrared digital count values associated with each of the five categories of fog occurrence in the study area are proposed. In addition, the height of the cloud base is computed for all processed SMS-2 data points, based on a formulation derived from radiation physics and empiricism available from the University of Wisconsin. Insofar as advancing the skill of objectively identifying marine fog areas from weather satellite observations is concerned, the results of this study are considered suggestive but not definitive, in part due to the limited data sample. The relation of the study to prior work at the Naval Postgraduate School, using NOAA polar-orbiting satellite data, is noted.

NAVAL POSTGRADUATE SCHOOL
Monterey, California

Rear Admiral Isham Linder
Superintendent

Jack R. Borsting
Provost

This thesis prepared in conjunction with research supported by the Naval Air Systems Command 370C.

Released as a
Technical Report by:

Approved for public release; distribution unlimited.

The Use of DMSP and SMS-2 Digital Satellite Data for Identifying Marine Fog in the Eastern North Pacific Ocean Area

by

Carl Bolton Ihli, Jr.
Lieutenant, United States Navy
B.S., United States Naval Academy, 1968

Submitted in partial fulfillment of the
requirements for the degree of

MASTER OF SCIENCE IN METEOROLOGY AND OCEANOGRAPHY

from the

NAVAL POSTGRADUATE SCHOOL
March 1977

ABSTRACT

Defense Meteorological Satellite Program (DMSP) and Synchronous Meteorological Satellite (SMS-2) digital satellite data, both visual and infrared, are processed and analyzed in context with transient/stationary synoptic ship reports, in an effort to identify areas of marine fog occurrence. The eastern North Pacific Ocean was chosen as the area of study; for various reasons the period was limited to 5-9 August 1976. Histograms and two-dimensional plots of visual and infrared data are generated as a function of five categories of fog/no-fog occurrence. Optimal ranges of visual and infrared digital count values associated with each of the five categories of fog occurrence in the study area are proposed. In addition, the height of the cloud base is computed for all processed SMS-2 data points, based on a formulation derived from radiation physics and empiricism available from the University of Wisconsin. Insofar as advancing the skill of objectively identifying marine fog areas from weather satellite observations is concerned, the results of this study are considered suggestive but not definitive, in part due to the limited data sample. The relation of the study to prior work at the Naval Postgraduate School, using NOAA polar-orbiting satellite data, is noted.

TABLE OF CONTENTS

LIST OF TABLES

Table

LIST OF FIGURES

ACKNOWLEDGEMENTS

The author would like to express his appreciation to Dr. Robert J. Renard, whose patient guidance and assistance were instrumental in the completion of the study.

Special thanks are extended to Mr. Steve Rinard and Miss Tanya Servaas, Department of Meteorology, Naval Postgraduate School (NPS) for their computer programming assistance, and to Mr. Mike McDermet and the personnel assigned to the Meteorology Laboratory, NPS, for their attention to the technical needs of the author.

Appreciation is also extended to the Naval Weather Service Detachment, Offutt Air Force Base, Nebraska, for providing DMSP digital satellite data and imagery for the study; to Fleet Numerical Weather Central, Monterey, California, and the Naval Weather Service Detachment, Asheville, North Carolina, for synoptic ship observations used in the study; to the personnel at the Space Science and Engineering Center, University of Wisconsin, particularly Mr. Gary Chatters, Mr. Fred Mosher, Mr. Tom Haig, and Mr. J. T. Young who were of great assistance in furnishing and advising on the use of the SMS-2 satellite data, and training on the MCIDAS; and to the National Environmental Satellite Service, Redwood City, California, for providing SMS-2 satellite imagery.

I. INTRODUCTION AND BACKGROUND

The occurrence of fog is a threat to all ocean-going vessels, civilian and military alike. In naval applications, aircraft operations as well as surface ship operations are affected by the visibility. A study concerning materiel dollar cost and, more importantly, losses of human life over a five-year period further emphasize the impact that marine fog has on naval operations (Wheeler, 1974).

Accurate depiction of fog regions over the open ocean on a real-time basis would be of significant value in any naval operation in which horizontal visibility is a limiting parameter. Ship routing, by way of example, would certainly take into account any reliable methods of fog diagnosis and prediction should such products exist.

Currently, only Fleet Numerical Weather Central, Monterey, California (FNWC) generates objective fog forecasts. Their product (FTER) forecasts fog occurrences for all areas of the Northern Hemisphere. FNWC promulgates the computerized probability of fog twice daily (0000 and 1200 GMT) for forecast intervals up to 72 hours. These forecasts are based on a statistical processing of certain model output parameters related to fog occurrence (U. S. Naval Weather Service Command, 1975).

The use of the meteorological satellite may lead to an improvement in diagnosing marine fog and concomitant

increases in predictive accuracy. Research conducted at the Naval Postgraduate School, Monterey, California (NPS) since 1974, made use of visual (VIS) and infrared (IR) weather satellite imagery from polar orbiting satellites to discern the presence of marine fog. Initial results indicated the need for further investigation into the use of digital satellite data in detecting marine fog (Wallace and Renard, 1975). Continuing investigations, using NOAA-2 digitized satellite data, established optimal ranges of count values for fog occurrence for both VIS and IR digital data (Hale and Renard, 1975). However, the level of skill in applying these findings indicated the need for follow-on research.

II. OBJECTIVES AND APPROACH

From the research cited in Section I there appeared to be two directions that future studies could take. One possible approach involved the analysis of more data observed by the same or another polar orbiting satellite. To this end the Defense Meteorological Satellite Program (DMSP) satellite was selected, largely due to its application for military oriented operations in general, and because its output will be eventually readily available to FNWC for operational purposes. Although the DMSP satellite is controlled by the United States Air Force, its products are in wide usage by Naval Oceanography and Meteorology Units as evidenced by the DMSP satellite installations at several land and afloat sites.

The second possible approach was to obtain data from a geosynchronous weather satellite and thereby have the additional advantage of nearly continuous coverage of an ocean area. This second option was also selected and the Pacific Ocean Synchronous Meteorological Satellite located over the equatorial Pacific Ocean area (SMS-2) was chosen.

Thus, the primary objective of the subject research is to ascertain the value and applicability of both DMSP and SMS-2 satellite data in identifying areas of marine fog over the open ocean.

The approach taken in pursuit of this objective was to statistically process and interpret DMSP and SMS-2 digital satellite data, with synoptic weather reports from transient and stationary ships used as "ground truth" verification. The immediate goal was to establish a limited range of VIS and/or IR digital count values which would allow fog/no-fog discrimination. In addition, usable statistical correlations of satellite and conventionally-reported weather parameters were sought.

III. DATA

A. AREA OF STUDY

The previously cited marine fog research conducted at NPS was confined to the North Pacific Ocean area. The area selected for this study, as dictated by the SMS-2 satellite coverage, was the eastern portion of that ocean, with the following boundaries: 30-60N; 115W-180. Although this area includes a portion of the west coast of the United States, only ocean areas were considered in the study (see Fig. 1).

B. TIME PERIOD FOR STUDY

The limiting factor in the determination of a time period of investigation proved to be the period for which the digital SMS-2 satellite observations could be obtained from the receiving site at the University of Wisconsin, Madison, Wisconsin. Initially, based on climatology and previous research, a period during the month of July was requested. July, climatologically, provides the highest frequency of fog occurrence over the North Pacific Ocean (Willms, 1975). Unfortunately, the month of July was pre-empted by another user. However, the period 1-15 August 1976 was available and arrangements were made for its acquisition. However, due to weather problems at Madison, Wisconsin, the receiving site was shifted to the Cambridge Research Laboratory, Cambridge, Massachusetts. Some

equipment difficulties at the east coast receiving station eliminated any data after 9 August 1976, so that SMS-2 data were available for the study only in the 1-9 August 1976 time frame.

DMSP data presented different problems. As had been advertised, DMSP data were made available from the United States Air Force Global Weather Central, Offutt Air Force Base, Nebraska, during the proposed 1-15 August time period. Unfortunately, the data as received at NPS did not cover the entire 15-day period. On some days data were unavailable; on other days either IR or VIS data, but not both, were available. On certain days when both VIS and IR data were available, the data in the study area were, in part, from various observation times differing by 12 or more hours or from the NOAA-4 satellite if DMSP data were missing.

Considering the limitations imposed on the study by both satellite systems and, after examining all data once received at NPS, a study period of only five days, 5-9 August 1976, was possible.

C. SYNOPTIC WEATHER REPORTS FROM TRANSIENT/STATIONARY SHIPS

Primary-time synoptic weather observations for 5-9 August 1976 were provided by FNWC in the main, with several missing synoptic times data available through archived data sources at the National Climatic Center (NCC), via the co-located Naval Weather Service Detachment (NWSD), at

Asheville, North Carolina. Surface ship synoptic reports established the basic "ground-truth" for the existence or non-existence of marine fog.

Initially, the four primary synoptic times of 0000, 0600, 1200 and 1800 GMT were considered. Later in the study it became necessary, due to other limitations, to consider only 0000 and 1800 GMT reports. The reason for this further limitation will be made apparent in a subsequent section.

Of the information available in a standard surface ship report all data were initially recorded in tabular format (see Fig. 2, for example). After filtering out reports that were outside the geographic limits of consideration, a total of 1335 ship reports were available at 0000, 0600, 1200 and 1800 GMT for the five-day study period. After the synoptic times 0600 and 1200 GMT were removed, a total of 825 ship reports were available for analysis.

D. DMSP SATELLITE DATA

DMSP digital data on magnetic tape were furnished by the Air Force Global Weather Central (AFGWC) at Offutt Air Force Base, Nebraska, through the auspices of the Naval Weather Service Detachment located there. Data as stored on the magnetic tape were depicted on the standard I-J grid, as used by FNWC. This grid is superimposed on a polar stereographic projection of the earth, true at 60 N latitude, with the pole at its center. It consists of 63 columns and 63 rows of equally spaced points. The I-J grid coverage

of the study area is included in Fig. 3. The distance between points on the grid is related to distance on the map by the map scale factor: 1 + sin 60°/1 + sin (latitude). This distance at 60 N is 206 nmi and reduces to 110 nmi at the equator.

There are a total of 64 by 64 DMSP data points (i.e. digital count values) within one single square of the I-J grid (Fig. 3) for a total of 4096 data points. The study area included 153 whole or partial I-J grid squares so that the total number of data points available at any one reporting time over the study area was very close to 600,000. Fig. 4 is a sample 64 x 64 grid of two-digit digital count values (DCV's). Table I summarizes the spacing of data points (data interval) within a unit I-J grid square as a function of latitude.

The digital data that appears at each of the data points in the 64 by 64 matrix ranges from DCV's of 0-63 indicative of 64 shades of grey for both visual (VIS) and infrared (IR) digital data. For VIS data, the lower DCV's represent areas with a very low albedo, such as the sea surface. In typical DMSP VIS imagery these surfaces appear very dark grey or black. Dense cloud layers, particularly cumulonimbus clouds, appear at the opposite end of the grey-shade spectrum as values in the high 50's or 60's. Due to the high albedo of such clouds, they appear nearly white on the DMSP VIS imagery.

For DMSP IR data, low DCV's and hence dark shades of grey are indicative of low temperatures while high DCV's indicate

relatively high temperatures. Because of this convention, the IR field is inverted prior to developing a positive print (IR imagery) so that the cloudy regions appear white, and thus relate well to that which the human eye is accustomed to viewing from the earth's surface. For both VIS and IR DMSP data a digital value of 63 represents missing data.

The data stored on magnetic tape were processed through the NPS computer facility and transferred to a print-out format for ease of accessing and extracting the required data. In order to access the data, ship latitude/longitude positions were converted to I-J grid coordinates. Once the I-J grid positions were known, data were easily extracted from the computer print-out. The formulae involved in the conversion from latitude/longitude to I-J coordinates were programmed on a hand-held programmable calculator and are included in Appendix A. I-J grid positions were calculated to the nearest hundredth so that an overlay subdivided accordingly could be used with each I-J grid square on the computer print-out.

An item of importance involved the accuracy of extracting a single point value from the available data. It was felt that an averaging scheme which took into account surrounding DCV's would be more representative than a single point value. Accordingly, two averaging schemes were used in determining average DCV's. The procedures involved in these averaging schemes are included in Appendix B. All

subsequent work with the DMSP VIS and IR data was accomplished using the "four by four" averaged parameters.

The most drastically limiting factor involved in extracting the DMSP data proved to be the time of observation. Since the DMSP satellite is polar orbiting, composite images and digital data covering the eastern North Pacific Ocean area were available only at specific times. Synoptic ship report times of 0000, 0600, 1200 and 1800 GMT in many instances did not coincide with times of satellite observation. It was decided to accept the DMSP observation as representative (in time) if it was within two hours of the actual synoptic time; data outside the two-hour limit was rejected. With this two-hour criterion, only 90 VIS and 196 IR reports could be matched to the original 1335 ship reports available during the five-day period. These totals further dwindled to 69 VIS and 116 IR reports with the limitations imposed by SMS-2 coverage to only the 0000 and 1800 GMT reports.

E. SMS-2 DATA

SMS-2 digital data were furnished on magnetic tape by the Space Science and Engineering Center (SSEC) of the University of Wisconsin at Madison, Wisconsin.

The digital count values range from 0 to 255 for both VIS and IR data. In the case of VIS DCV's, low (high) numbers correspond to surfaces having low (high) albedo, while for IR data relatively high (low) temperatures appear as low (high) DCV's. It would be expected, therefore, that a

cloud mass with considerable vertical development, such as a cumulonimbus tower, would exhibit both VIS and IR values at the upper end of the count value range. The overall range of DCV's encountered in this study was 36-196 for VIS data and 73-197 for IR data.

The nominal accuracy of SMS-2 VIS data is one-half nmi by one-half nmi at the subsatellite point (vicinity of Equator, 135W). Actual values of line and element spacing at full resolution as a function of latitude/longitude position are included in Fig. 5. The variation of line and element values as one proceeds poleward and either eastward or westward of the subsatellite point should be noted. The stated SMS-2 accuracy is dependent upon many parameters such as satellite spin rate, satellite attitude, orbit eccentricity, camera geometry, orbit precession, and height above the earth's surface. Data resolution of two nmi by two nmi (i.e. 1/4 nominal VIS resolution) was considered adequate and therefore used in the processing of all VIS data, thus greatly reducing the quantity and cost of data to be processed.

Reference has been made to line and element values when addressing the SMS-2 data. Lines and elements merely refer to the manner in which SMS-2 data are recorded on magnetic tape or displayed on a data print-out. Each VIS or IR DCV is identified or indexed with an associated line and element number pair that uniquely locates the DCV on a projection of the earth's surface. Line and element orientation are depicted on a map of the study area in Fig. 6. It must be

emphasized, however, that line and element orientation are functions of satellite geometry and hardware and are, thereby, not a direct function of parallels of latitude or meridians of longitude on the earth's surface. The two nmi by two nmi data available for this study represent averages of four data elements along every fourth line.

SMS-2 IR data resolution is two nmi by four nmi. In the format mode available to the study, data are spaced at two nmi along each line with each line duplicated once to standardize the VIS and IR data depictions to a two nmi by two nmi interval. Sample VIS and IR data are included in Figs. 7 and 8, respectively.

In addition to the DCV data on magnetic tape, the SSEC furnished a print-out of corresponding line and element values at ten degree latitude/longitude increments. Thus, an interpolation scheme was necessary to match the ship's latitude/longitude positions (to the nearest tenth) to the corresponding line/element values. The solution appeared to be in the use of the natural bicubic spline curvilinear interpolation scheme available at the NPS Computer Center library. Using this routine, line and element values could be interpolated to the nearest whole degree of latitude/longitude and linearly interpolated thereafter for finer accuracy.

Interpolation using the bicubic spline was successfully attempted but the processing time involved appeared

prohibitive, especially since the temporal change of all satellite variables also necessitated a new calculation of line and element grids for each new synoptic time. With this realization, it became evident that data processing via these methods was far too time consuming and an alternate method for handling the data was sought.

The processing problem was resolved by extracting the data required for the study at the SSEC using the Man-Computer Interactive Data Access System (MCIDAS) (see Appendix C). Accordingly, for four days during the latter part of December 1976, the author processed data at the SSEC using the MCIDAS. The accessing of required data via line and element number indices proved to be a simple task with the MCIDAS.

Having read in the magnetic tape, an analog image of the digital data was generated on one of the MCIDAS terminals. Once the "satellite picture" was generated, certain geographic features (i.e. landmarks) on the earth were identified and their known latitude/longitude positions were compared to latitude/longitude positions that had been transformed from the satellite data. For the eastern North Pacific Ocean, few landmarks were available and were, of necessity, located at the periphery of the study area or even further inland on the continent. Landmarks that were consistently visible during the 5-9 August time period included Isla Angel de la Guarda in the Gulf of California, the Great Salt Lake in Utah, Santa Rosa Island off the

southern California coast, and a noticeable feature in the Great Lakes region. During the study period, none of the islands in the Aleutian Chain could be used as landmarks because of the cloud cover consistently over that region.

For purposes of this study, maximum navigational errors of 10 nmi were deemed acceptable. When navigation information was checked for each of the four synoptic times in the five-day period, the SMS-2 data at 0600 and 1200 GMT were consistently outside acceptable tolerances while 0000 and 1800 GMT could be adjusted to within the 10 nmi criterion. In addition, at synoptic times 0600 and 1200 GMT (night-time in the study area) SMS-2 IR data only were available. Thus, the deicison was made to set aside the 0600 and 1200 GMT data and continue processing only the 0000 and 1800 GMT VIS and IR data. At this point, the conventional data set was reduced to 825 available ship reports. Navigational adjustment procedures as alluded to above will not be discussed herein due to the detail involved.

Once the navigation problem was solved, extraction of necessary digital count value data was a simple matter. Rather than extracting a single point value of VIS or IR data, 11 x 11 matrices of DCV's were printed out for each transient ship latitude/longitude position, one matrix each for the VIS and IR data, respectively. Simple averages of the eight count values surrounding the center value plus the center point value were also performed. These "nine-point" averages were used in subsequent statistical analyses.

Weighted averages as used with the DMSP data were not computed due to time limitations (see Figs. 7 and 8).

Another important parameter that was derived based on SMS-2 DCV's was one involving cloud heights. This parameter was available through MCIDAS processing and was extracted for each ship latitude/longitude position. A brief discussion of the MCIDAS Cloud Height (CLDHGT) program (Mosher, 1974), as it applies to this study is included in Appendix C.

IV. DATA ANALYSIS AND RESULTS

A. APPROACH

The organization of data was based on ground-truth ship report positions at 0000 and 1800 GMT for the five-day period 5-9 August 1976. A sample data tabulation is included in Fig. 2.

The analysis of the fog/no fog data was related to a parameter developed in marine fog research at the NPS (Renard, et al, 1975; Willms, 1975), namely the fog duration category (FDC). Fog duration categories (FDC's) were manually determined for each of the synoptic ship reports based on unique combinations of visibility plus present and past weather. Willms' classification scheme, based on the visibility weather group elements, is included in Table II. 24 of Willms' 39 possible FDC's are represented in this study. Since the data set was not significantly large, it was decided to combine the FDC's into five groups for further processing (see Table III). At this point, the general approach was to examine the available data with the FDC parameter acting as the common basis of comparison. When the SMS-2 data processing was completed, 718 data points could be matched to the 825 synoptic ship reports available.

B. DMSP DATA ANALYSIS AND RESULTS

As previously indicated, the size of the DMSP data set was very small. Of 718 ground truth ship reports available,

69 VIS and 116 IR DMSP digital count values were available for analysis. Using a histogram representation, results are presented in Figs. 9 through 12. For histograms that were generated through the NPS computer facility, such as Figs. 9 and 11, a plotted empirical density function (F) is included. A line through the "F" points essentially gives a smoothed profile of the frequency data. In addition, histogram percentage frequencies are indicated on the ordinate and the mean value of each distribution is indicated by a vertical column of "M's". Table IV summarizes the results concerning the distribution of DMSP digital values.

The IR distribution (Fig. 11) appears to approach a normal distribution to a much greater degree than does the VIS counterpart (Fig. 9), but lack of sufficient data makes such a conclusion very tenuous. The range of VIS DCV's (26 - 60) is somewhat greater than that for IR DCV's (19 - 46) with the distribution more erratic for the former. Similar observations are appropriate when considering each of the FDC's in Figs. 10 and 12 and Table IV.

C. SMS-2 DATA ANALYSIS AND RESULTS

1. SMS-2 VIS and IR DCV Analysis - Histograms and Scatter Diagrams

The SMS-2 data set proved to be more informational than the DMSP data, due in part to the significant increase in size of the data set. It must be emphasized, however, that when dealing with a sample size numbering 718, statistical findings are necessarily more indicative or

suggestive than truly definitive as compared with a sample size numbering say, 10,000. With this caution in mind, results of the analysis of the SMS-2 data follow.

As in the case of the DMSP data, all SMS-2 data, VIS and IR separately, were organized into the same five groups of FDC's. Figs. 13 and 19 depict the distributions of VIS and IR average DCV's respectively, for all data. Average count values were selected as more representative than point values. However, average count value distributions were not significantly different from their point-value distribution counterparts. As had been observed with the DMSP data, a difference in range interval was noted in VIS as opposed to IR data. VIS data encompassed 159 possible values while IR data spanned 123 possible digital count values. In fact, for all groups, except FDC GR 2, the IR DCV ranges are less than those observed for their VIS counterparts. It was also interesting to note that the absolute minimum/maximum count values encountered were 36-198 for VIS and 73-196 for IR; possible SMS-2 digital count values are advertised to range from 0-255.

After the entire data set had been scrutinized on the initial two plots, additional histograms segregating the data into the FDC groups were constructed and appear as Figs. 14 through 18 and 20 through 24. Additionally, Table V summarizes the essential statistics from all of the SMS-2 histogram data. The following additional observations were made based on the histograms:

(1) Fog reports seldom occur in the VIS count value range of approximately 36-72 (i.e. low albedo)(see Figs. 14 through 17).

(2) Similarly, fog reports seldom occur in the IR count value range of 73-89 (i.e. relatively high temperatures)(see Figs. 20 through 23).

(3) Limiting values, similar to (1) and (2) above, at the upper end of the VIS (high albedo) and IR (low temperature) count value range are not evident.

(4) Mean DCV's differ little in all categories associated with fog for both VIS and IR data (Table V).

The presentation of any one parameter as a function of FDC groups was, in essence, a one-dimensional view of the data. To further pursue a solution to the basic objective of the research, a multi-dimensional data depiction method was desirable. Accordingly, two-dimensional plots were constructed with VIS and IR DCV's as the two axes. For each ground-truth ship latitude/longitude position, the VIS average DCV was plotted versus the IR average DCV. Five plots were generated (Figs. 25 through 29) which segregated the data into the five FDC groupings previously defined. Information depicted on these plots was identical to the histogram data but allowed VIS and IR data to be "spatially" correlated.

Objective analysis techniques employed up to this point had still not established any limited range of either

VIS or IR count values for fog occurrence. In an effort to establish an upper cut-off range of VIS/IR values for fog occurrence (to supplement the limiting low values already determined) a subjective analysis technique was selectively employed using both VIS and IR satellite imagery. The principle involved examination of all data locations, except those associated with FDC 180 (no fog) on the VIS/IR imagery in an effort to segregate out those reports in which middle and/or high clouds were in evidence. This step did not negate surface-based observations of fog but merely identified those ship locations where the satellite was seeing a low cloud type (as stratus) only.

The accomplishment of this subjective "sanitization" proved the necessary breakthrough in establishing reasonable cutoff boundaries for the IR count values. Figs. 30 through 33 depict the "sanitized" count-value distributions for the fog-associated FDC groups. A comparison of these figures with the immediately preceding set (Figs. 25 through 28) graphically illustrates the significant decrease in IR count value range. Table VI summarizes SMS-2 count value parameters before/after the subjective sanitization procedure. It is important to note the relatively small change in the VIS range of count values as compared to the IR range. Results observed are reinforced to some degree by the findings of Hale and Renard in their 1975 study which utilized NOAA-2 digitized data in diagnosing marine fog. A large VIS range of possible DCV's and a much more limited range of IR count values were reported in their study.

During the selective sanitization of the ship latitude/longitude positions, it was observed that a certain number of reports when viewed on the VIS/IR imagery appeared to be in areas of large gradients of grey shade values, and hence the interpretation became critically dependent on gridding and navigational accuracies as well as on the observation itself. Two examples are included here to illustrate the high observed correlation between imagery and associated digital data.

The first example, depicted in Fig. 34, is from 0000 GMT data on 5 August 1976. The VIS and IR imagery at the ship latitude/longitude position indicated a uniform layer of low clouds with several localized middle and/or high cloud patches surrounding the ship position. The VIS data matrix reflects this condition quite accurately in the strong count value gradients extant across the data matrix. The IR data matrix, due primarily to resolution differences, does not exhibit the gradient as well except at the right edge of the matrix. To further confirm the satellite data, the synoptic ship report indicated fractostratus reported for low cloud type and double-layered altocumulus and dense cirrus in patches for the middle and high cloud types respectively. The dimensions of the SMS-2 VIS/IR data matrices (Fig. 34) are approximately 17 nmi (approximately east/west) by 32 miles (approximately north/south).

The VIS and IR data depicted in Fig. 35 correspond to an area on the VIS imagery that constituted a "clear slot"

crossing precisely at the ship latitude/longitude position indicated. The strong count value gradients observed on either side of the slot indicate the presence of highly reflective clouds. The IR data does not reflect this "clear slot" probably due to the previously mentioned resolution differences and the resultant "smearing" of the digital data. VIS/IR data matrix dimensions at the geographical position are approximately 20 nmi (approximately east/west) by 32 nmi (approximately north/south).

2. SMS-2 Cloud Height Parameters

Since the histogram approach of data presentation had proved its utility, it was employed again in an effort to glean some meaning from the SMS-2 cloud height parameters which had been generated using a program developed by Mosher at the University of Wisconsin (Mosher, 1974). As discussed in Appendix C, the parameter of interest was the derived height of the cloud base. Included in Figs. 36 through 41 are histograms of cloud base height in meters (abscissa) as a function of the various FDC groups previously defined. The CLDHGT program had not been developed for application in fog research and hence was not specifically "tuned" to necessarily provide cloud base heights near zero as one observes with fog. Some of the assumptions inherent in the CLDHGT program such as the development and tailoring of the model to cumulus-type clouds obviously would affect generated results. It was not a great surprise then, that negative heights were generated using the CLDHGT program.

Perhaps the most meaningful inference drawn from the cloud height histograms is the near Gaussian distribution (without regard to negative cloud heights) observed particularly in Figs. 36, 37 and 39. It should be noted that mean cloud base heights calculated for each of the fog groups were, in each instance, less than the mean height calculated for the FDC 180 (no fog) group. Table VII summarizes essential results from the CLDHGT program.

The full impact that a satellite-generated cloud height program might have in achieving the goals stated for this study cannot be answered by this research. Further investigation, refinement, and possible "tuning" of the CLDHGT program for this application to marine fog should be accomplished.

3. Other Statistical Relationships

To supplement the fog study investigation without specific application of the digital satellite data, weather parameters available in the standard synoptic ship report were also statistically examined. Using the histogram approach again, air temperature, sea surface temperature, and surface wind direction were depicted as functions of the various FDC groups. The parameter that proved most interesting was the distribution of the surface wind as a function of FDC. The surface wind distribution for those data in category FDC GR 1 will be specifically addressed here.

In examining the histogram initially (Fig. 42), some two-thirds of the wind reports fell between directions

150 and 270 deg. To depict the surface wind data in a second fashion and to also indirectly involve the VIS and IR DCV's, wind directions were attached to each of the data points depicted in Fig. 31. To establish mean wind directions, averages by column and row as portrayed in Fig. 43 were performed. For the averages given in which five or more wind reports were considered in the average, the mean wind directions were as follows: 160 through 262 along the VIS axis; 171 through 226 along the IR axis. Thus, the surface winds with southerly components are typically related to heavy fog conditions over the eastern North Pacific Ocean during the August period studied.

V. CONCLUSIONS AND RECOMMENDATIONS

The principal objective of this study was to ascertain the value and applicability of DMSP and SMS-2 satellite data in the diagnosis of marine fog over the open ocean. Through the interpretation and processing of digital data from both satellite systems with conventional surface ship reports as ground-truth verification, optimal ranges of digital count values related to fog occurrence for both the VIS and IR data were determined (Table VI). A secondary objective of the study, the establishment of usable statistical correlations of satellite and conventionally-reported weather parameters, was only partially achieved through the relationship between observed fog reports, associated surface wind, and SMS-2 VIS and IR DCV's. Further statistical analyses were not performed using these data due to time limitations.

DMSP data proved insufficient in quantity for truly meaningful input to the study as a whole. Any polar orbiting satellite data utilized in a study such as this one must be available over a much longer time period so that a representative number of data points may be made available for investigation. Processing techniques employed herein, however, may be useful for future studies involving DMSP data.

SMS-2 recorded data processed using the MCIDAS, provided the major data source for the study. The high quality

numerical products and imagery available from the SMS-2 system provided the necessary base for meaningful data processing. Even though the final sample size for the study was relatively small, the processing accuracies attained throughout the investigation were noteworthy and provided very high quality data for further analysis. The utility of a derived cloud height parameter that has been finely tuned to account for various cloud types and varied atmospheric conditions is apparent. Although the MCIDAS CLDHGT parameters derived for this study did not provide significant insight into fog diagnosis, it is felt that refinement and development of this program will provide valuable input toward future studies. Perhaps the CLDHGT program will also be able to address still another problem, namely, the segregation and discrimination of fog from stratiform clouds without associated fog.

The following recommendations are offered for future studies:

(1) Conduct a similar study for a longer time period using both DMSP and SMS-2 data.

(2) Work toward increased automation of processing techniques herein outlined using existing computer facilities.

(3) Investigate the feasibility of modifying existing MCIDAS navigational and CLDHGT programs for use on the NPS computer.

(4) Further investigate the MCIDAS CLDHGT program as developed by Mosher (1974) in the fog diagnosis application.

(5) Further examine statistical relationships between conventional synoptic ship report data and VIS/IR count value distributions.

(6) Consider future fog research using the MCIDAS facility at the SSEC, University of Wisconsin.

(7) Investigate a scheme which would involve the assignment of "weighting factors" to selected VIS/IR digital count value parameters and when used in combination with climatology, moisture content, temperature, wind, and other fog-related parameters, arrive at a credible fog probability analysis (Hale and Renard, 1975).

APPENDIX A

Conversion of latitude/longitude position to I-J grid coordinates (FNWC Subroutine Library).

The following expressions were programmed for use with a programmable calculator:

$$I = I_p + [(Re)\ (\frac{\cos\ \phi}{1 + \sin\ \phi})\ (\cos(350-\lambda))]$$

$$J = J_p + [(Re)\ (\frac{\cos\ \phi}{1 + \sin\ \phi})\ (\sin(350-\lambda))]$$

where:

I_p = Pole position = 31

J_p = Pole position = 31

ϕ = Latitude, in degrees

λ = Longitude, in degrees

Re = Distance from pole to equator in grid mesh lengths = 31.205.

APPENDIX B

Averaging schemes for DMSP digital data - 2x2 and 4x4.

Given:

(1) Set of I-J grids computer produced, each consisting of 64 by 64 (4096 total) digital count values.

(2) Latitude/longitude positions converted to I-J grid coordinates (see Appendix A).

(3) Overlay, subdivided to nearest hundredth, to extract values from printed grid.

Procedure:

(1) Enter I-J grid (with overlay) and select the two-digit value closest to point on the overlay.

(2) Extract surrounding four points (including point value just selected); sum points and divide by four for 2x2 average.

(3) For calculation of the 4x4 average a weighting scheme is used, based on radial distance from the center of the grid. I-J coordinates entered are assumed to be at grid center to accomplish this average.

Points a, b, c refer to digital count values as located on 64x64 grid.

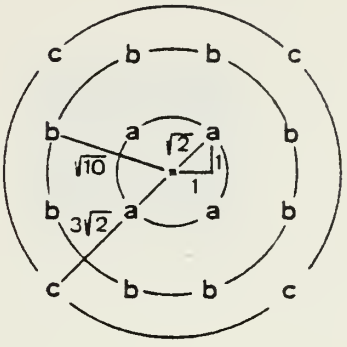

Assume: Distance between elements is equal to two units for purposes of deriving weighting factors (W_r), (i.e. distance a to b = 2 units).

$$W_a = \frac{1}{\sqrt{2}} \qquad W_b = \frac{1}{\sqrt{10}} \qquad W_c = \frac{1}{3\sqrt{2}}$$

therefore, $$\Sigma W_r = 4\left(\frac{1}{\sqrt{2}}\right) + 8\left(\frac{1}{\sqrt{10}}\right) + 4\left(\frac{1}{3\sqrt{2}}\right)$$

$$\Sigma W_r = 6.301058$$

Weighting Factors:

at all points "a" = $\frac{W_a}{\Sigma W_r} = \frac{\frac{1}{\sqrt{2}}}{6.301058} = \underline{.1122203}$

at all points "b" = $\frac{W_b}{\Sigma W_r} = \frac{\frac{1}{\sqrt{10}}}{6.301058} = \underline{.0501864}$

at all points "c" = $\frac{W_c}{\Sigma W_r} = \frac{\frac{1}{3\sqrt{2}}}{6.301058} = \underline{.0374067}$

CHECK: Does $4\left(\frac{W_a}{\Sigma W_r}\right) + 8\left(\frac{W_b}{\Sigma W_r}\right) + 4\left(\frac{W_c}{\Sigma W_r}\right) = 1$?

$$4(.1122203) + 8(.0501864) + 4(.0374067) =$$

$$.9999997 \approx 1$$

Sample Averaging Procedure:

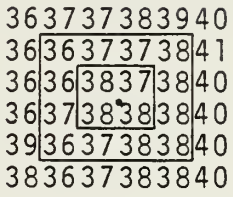

"•" = Exact location of I-J coordinate (to nearest hundredth)

point value = 38

$$\text{2x2 average} = \frac{38 + 37 + 38 + 38}{4} = 37.8$$

4x4 average = .1122203(38 + 37 + 38 + 38) +

.0501864(37+37+38+38+38+37+37+36)

+ .0374067(36 + 38 + 38 + 36)

= 37.4

APPENDIX C

The Man-Computer Interactive Data Access System (MCIDAS)

The Man-Computer Interactive Data Access System (MCIDAS) located at the Space Science and Engineering Center at the University of Wisconsin, Madison, Wisconsin, was developed for processing two dimensional image data from high volume data sources such as the Synchronous Meteorological Satellite (SMS-2) which transmits approximately 75 billion bits of image data each day (Smith, 1975). The characteristics that are required for a system to process SMS-2 data and which were therefore built into the MCIDAS include:

> "a. Best possible navigation
> b. Preservation of inherent resolution and geometry
> c. Speed and precision of automated techniques
> d. Human interaction only for decision-making but not for data handling or measurement
> e. Combination of digital and analog hardware
> f. Real or near-real time processing."
>
> (Chatters and Suomi, 1975)

Some of the capabilities of the MCIDAS include the following:

(1) Digital data may be transformed into analog picture format display at MCIDAS terminals.

(2) Images may be time sequenced on a terminal; a useful capability in tracking clouds.

(3) Inherent in the system's operation is an interactive capability in which the human operator always occupies a decision-making position.

(4) Images (pictures) on a MCIDAS terminal may be combined or overlaid as well as color enhanced.

Unique features which are intrinsic to the MCIDAS include both a unique navigational model and the WINDCO/CLDHGT system. The navigational model, although extremely complex, allows rapid transformation from satellite coordinates to true earth coordinates. The WINDCO/CLDHGT system was developed for use in cloud-tracking.

For this study, the CLDHGT sub-system provided a unique parameter: cloud base height derived from satellite digital data. The basic steps involved in the program include the following:

(1) Using visible brightness values the optical thickness of a cloud is determined.

(2) From the optical thickness, the IR emissivity of the cloud is computed.

(3) The true temperature of the cloud is then computed.

(4) From this temperature, and climatological soundings indexed by season and geographical position, the height of the cloud top is determined.

(5) Cloud thickness can be computed from the optical thickness and an extinction coefficient (Mosher, 1974).

Cloud thickness was subtracted from cloud top height to produce a cloud base height for each ground truth ship latitude/longitude position. Since the program was originally developed and modeled for cumulus-type clouds, a tentative correction factor was introduced by Mr. Mosher for the purpose of this study.

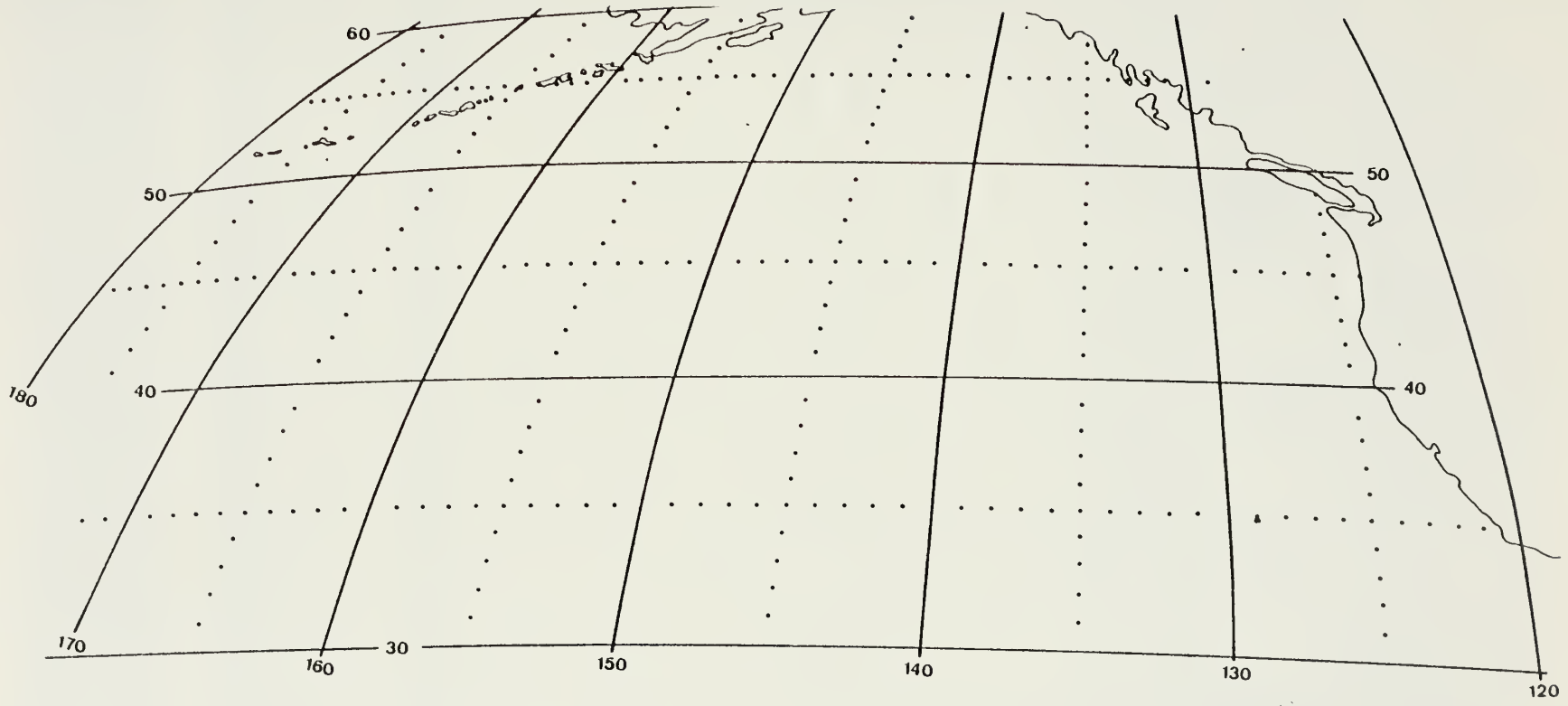

Figure 1. Study area.

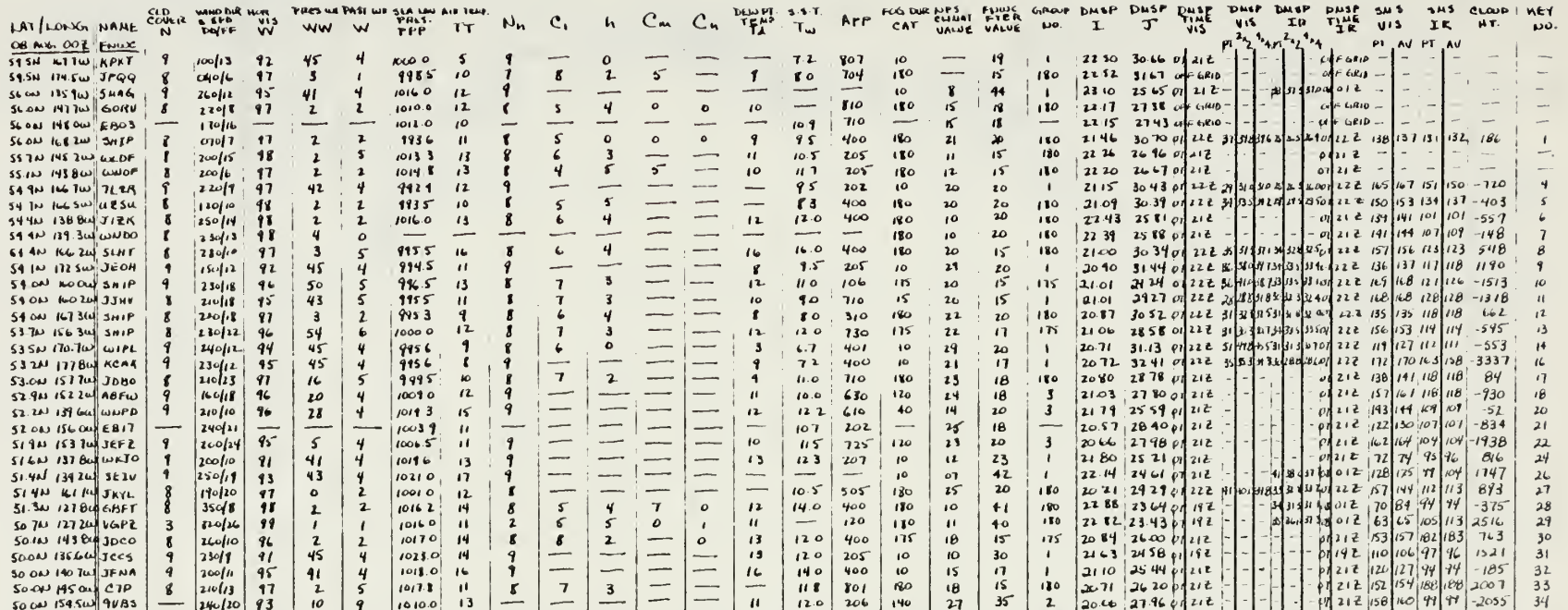

Figure 2. Sample tabulated data, 0000 GMT, 8 August 1976.

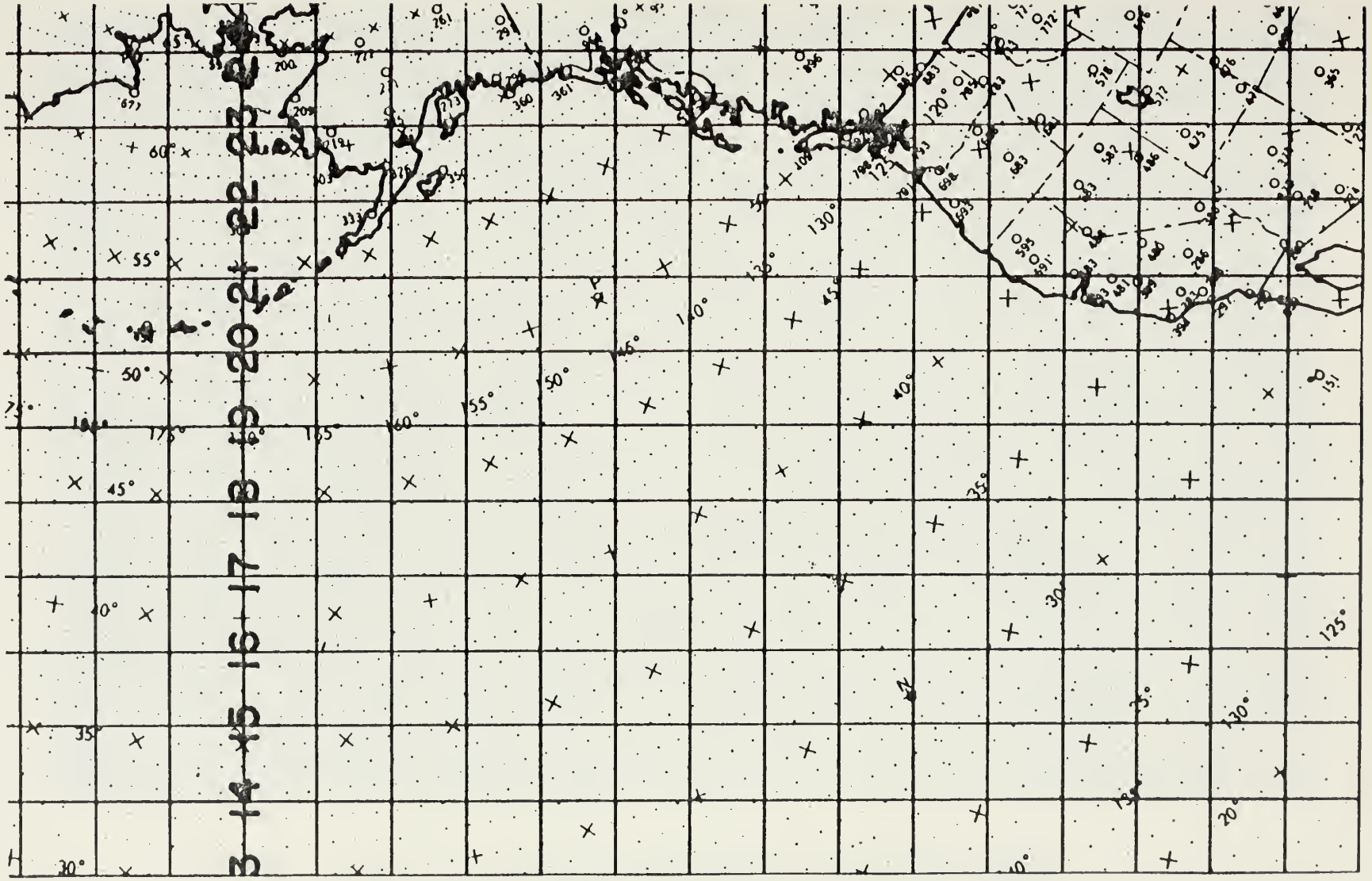

Figure 3. I-J grid coverage of study area.

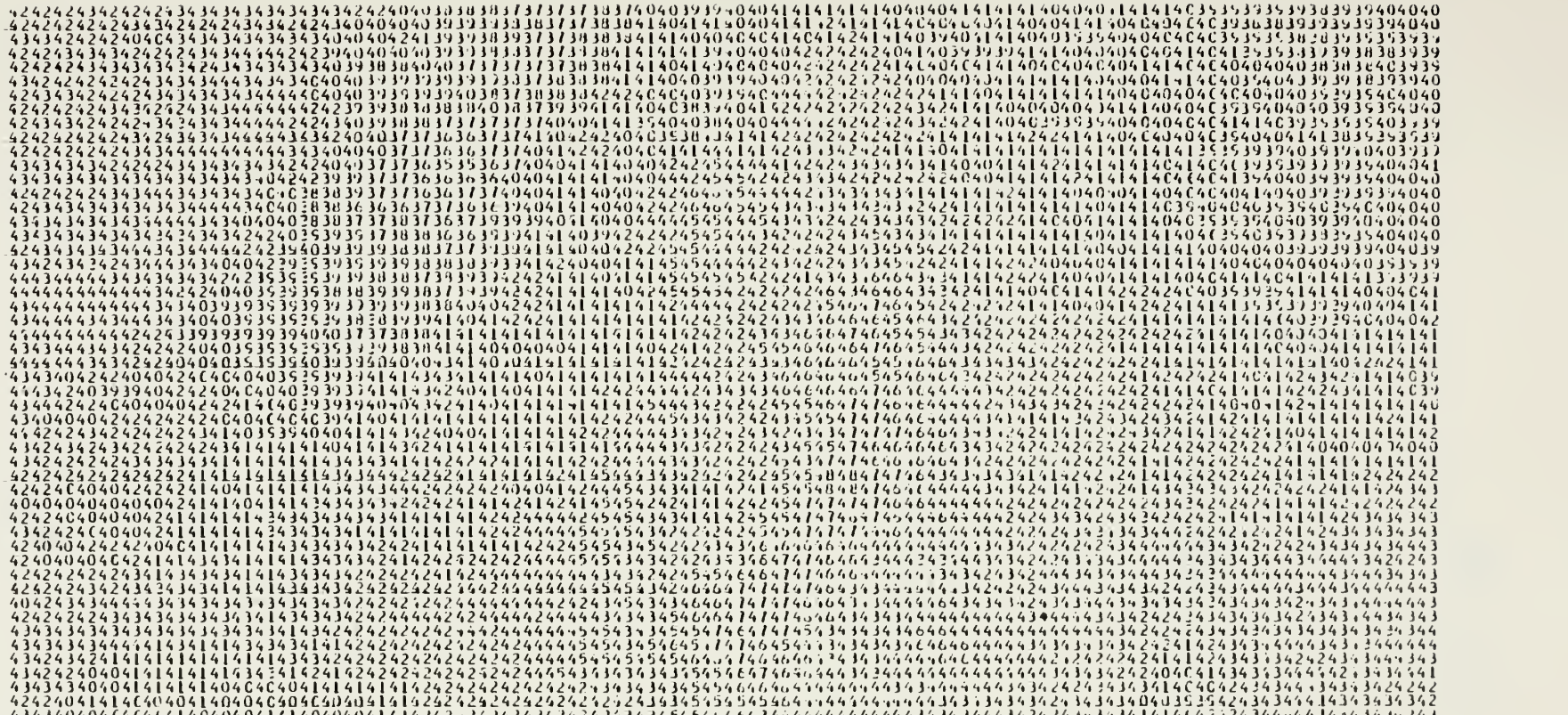

Figure 4. 64 by 64 grid of DMSP IR digital count values (Each count value is two digits) for 1300 GMT 9 August 1976.

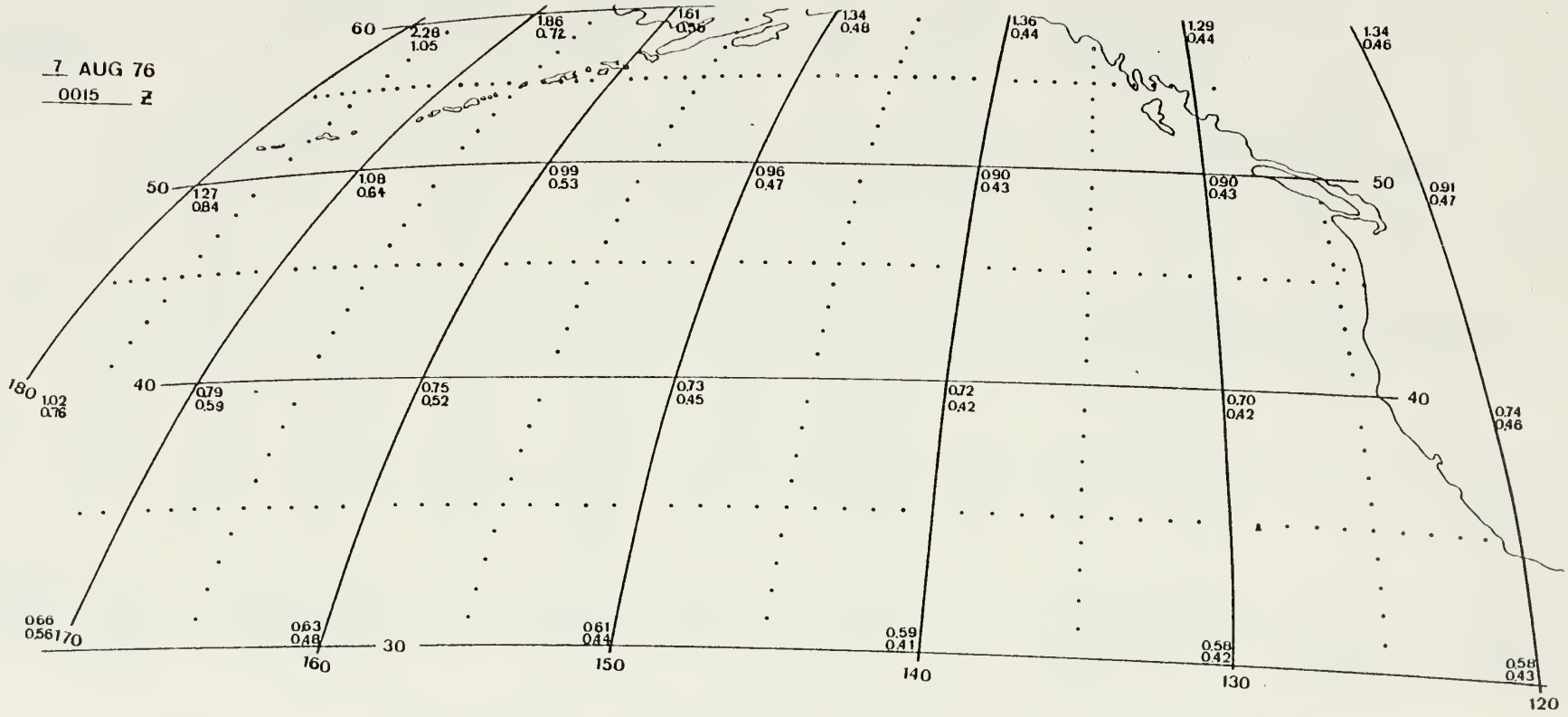

Figure 5. Line (top number) and element (lower number) spacing (nmi) as a function of latitude/longitude position (sample at 0015 GMT, 7 August 1976).
(Note: Element values along 170W and at 40N 180 are interpolations necessitated by a computer software error.)

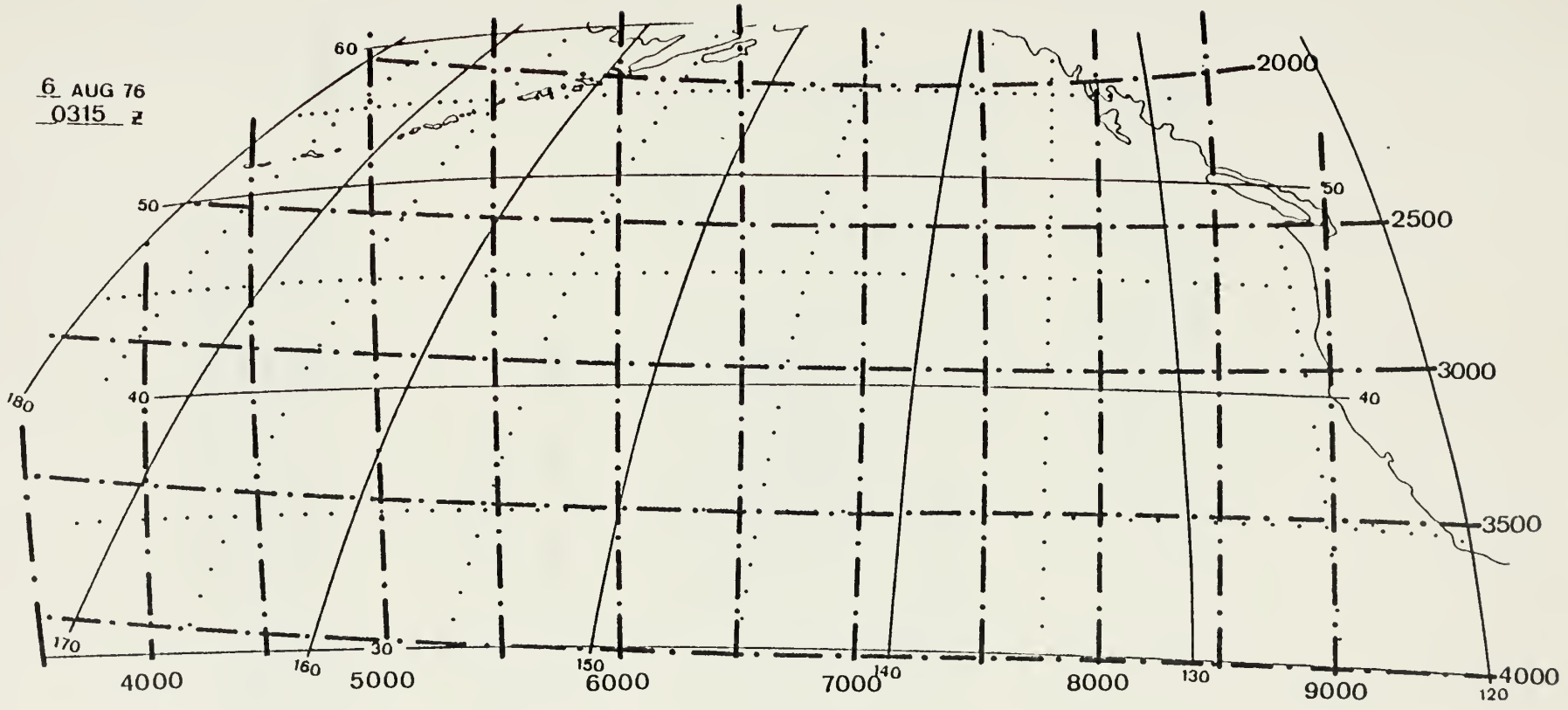

Figure 6. Isolines of SMS-2 line value (2000-4000) and element value (3500-9000) projected on a SMS-2 mapping of the study area, 0315 GMT, 6 August 1971.

START COORD LINE=2177 ELE=6669

LAT=493829 LON=-1454929

DAY=1876220 TIME=1500

137	118	138	138	140	144	145	144	147	147	153
108	123	134	145	150	141	138	138	148	147	150
121	135	141	145	153	141	134	141	152	151	146
125	130	143	149	147	134	140	145	152	148	149
124	140	142	144	141	138	142	152	154	149	146
128	136	141	145	140	(150)	151	147	145	144	140
142	147	147	154	144	147	151	142	137	145	151
137	142	154	144	135	145	147	138	141	141	140
151	145	137	125	133	148	147	139	141	140	131
143	133	131	138	145	138	137	143	129	134	127
146	139	131	145	124	126	138	123	121	127	125

END COORD LINE=2217 ELE=6709

LAT=490128 LON=-1451429

Figure 7. Sample SMS-2 grid of VIS digital count values (DCV's); center value (circled) is at ship latitude/longitude position; boxed area includes nine points used to obtain average DCV.

START COORD LINE=2175 ELE=6669

LAT=494019 LON=-1454955

DAY=1976270 TIME=1500

95	94	94	94	95	95	95	96	101	99	100
95	95	96	96	96	96	99	99	100	101	101
95	95	96	96	96	96	99	99	100	101	101
96	98	98	98	98	99	99	100	100	100	100
96	98	98	98	98	99	99	100	100	100	100
98	98	98	99	99	100	100	100	99	99	99
98	98	98	99	99	100	100	100	99	99	99
98	98	98	99	99	99	99	98	99	107	108
98	98	98	99	99	99	99	98	99	102	103
98	98	98	98	98	95	97	97	98	99	105
98	98	98	98	98	95	97	97	98	99	105

END COORD LINE=2215 ELE=6709

LAT=490314 LON=-1451457

Figure 8. Sample SMS-2 grid of IR digital count values (DCV's); center value (circled) is at ship latitude/longitude position; boxed area includes nine points used to obtain average DCV.

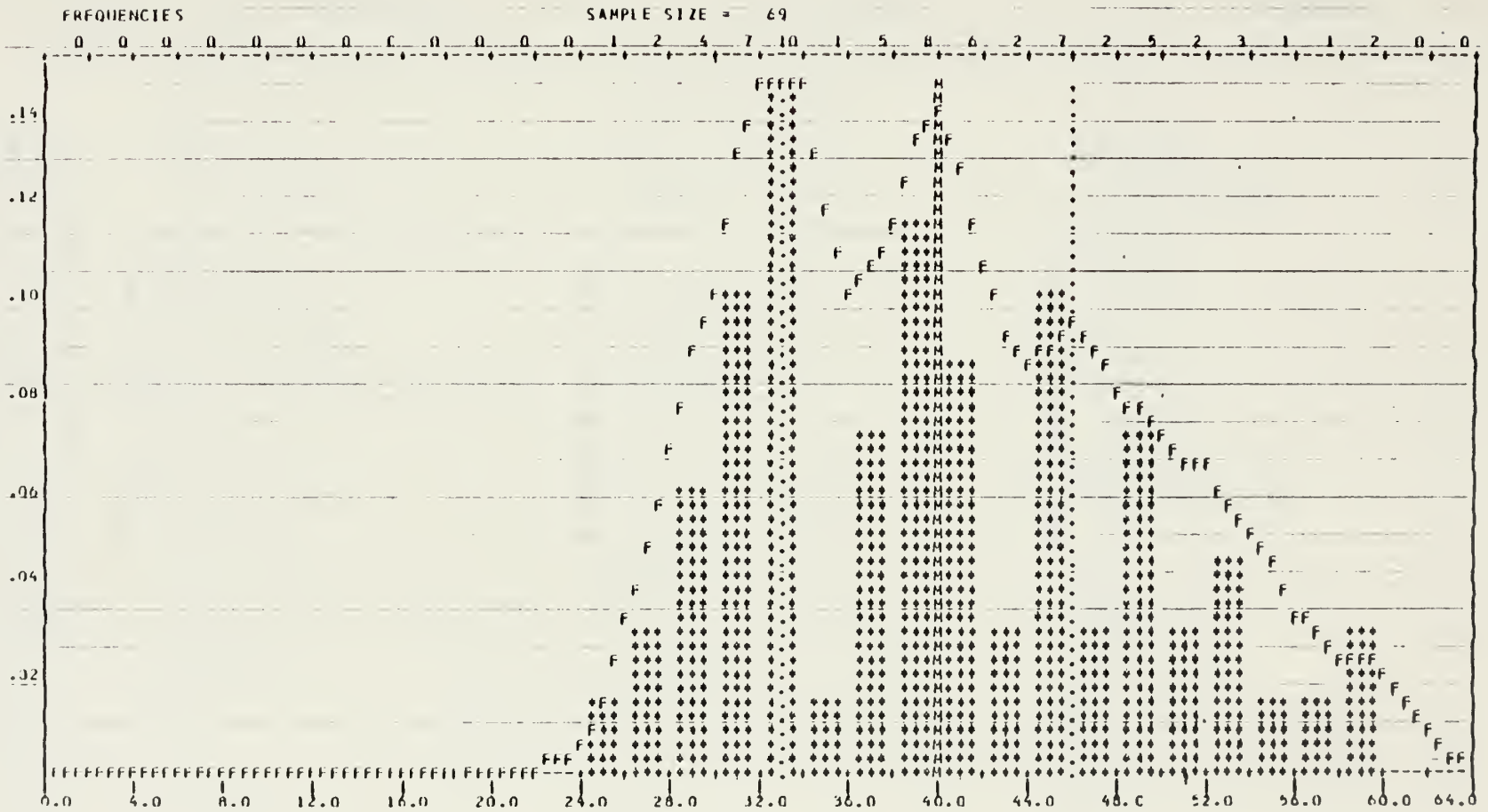

Figure 9. Frequency distribution of DMSP VIS average digital count values (DCV's) for all fog duration categories (see Tables II and III); 30-60N, eastern North Pacific Ocean, 5-9 August 1976; (1) frequencies and sample size along abscissa (top), (2) percentage frequencies along ordinate, (3) M = mean DCV, (4) F = empirical density function.

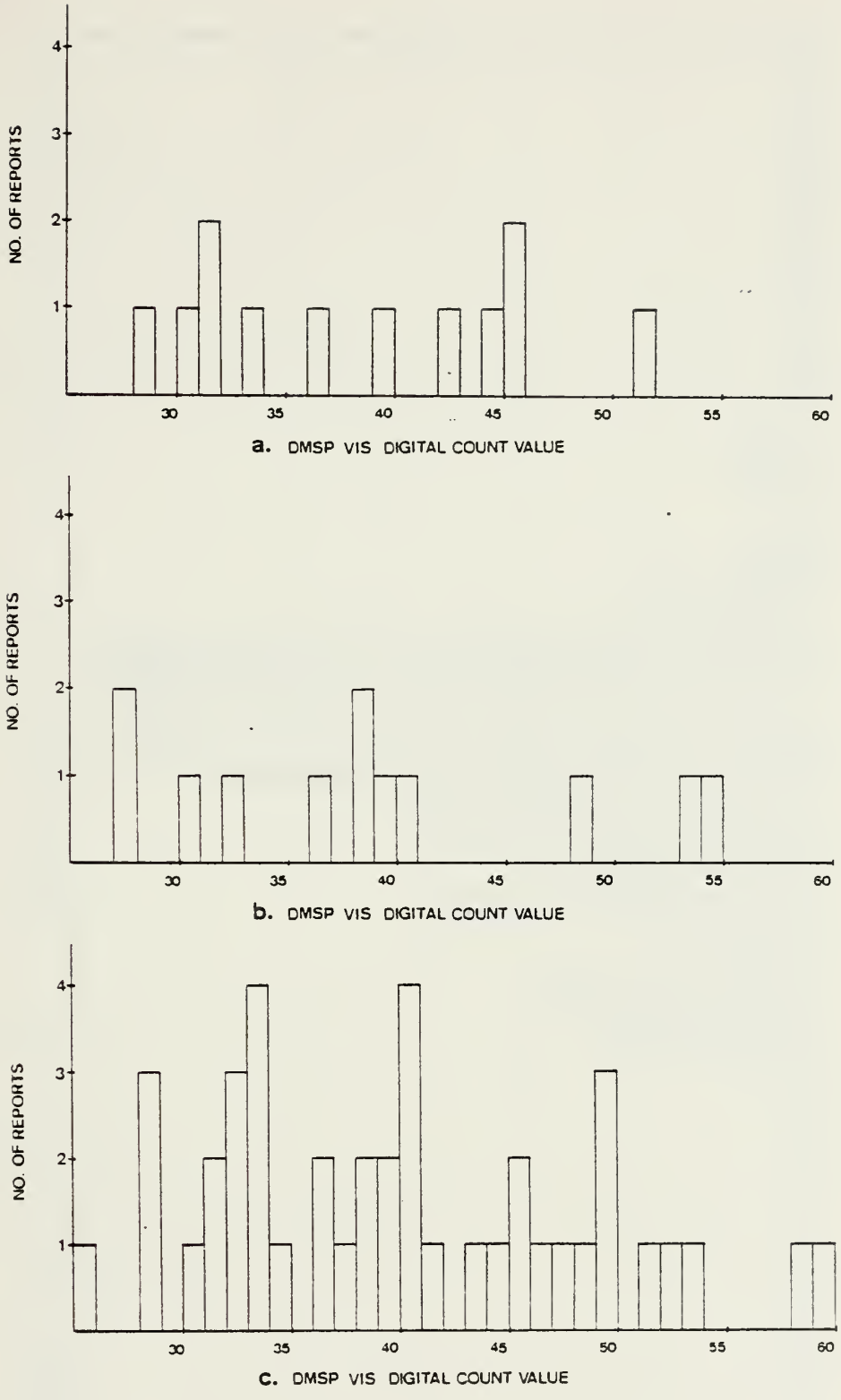

Figure 10. Frequency distribution of DMSP VIS average count values for: (a) FDC GR 1; (b) FDC GR 2, FDC GR 3, and FDC 175; (c) FDC 180 (see Tables II and III); 30-60N, eastern North Pacific Ocean, 5-9 August 1976.

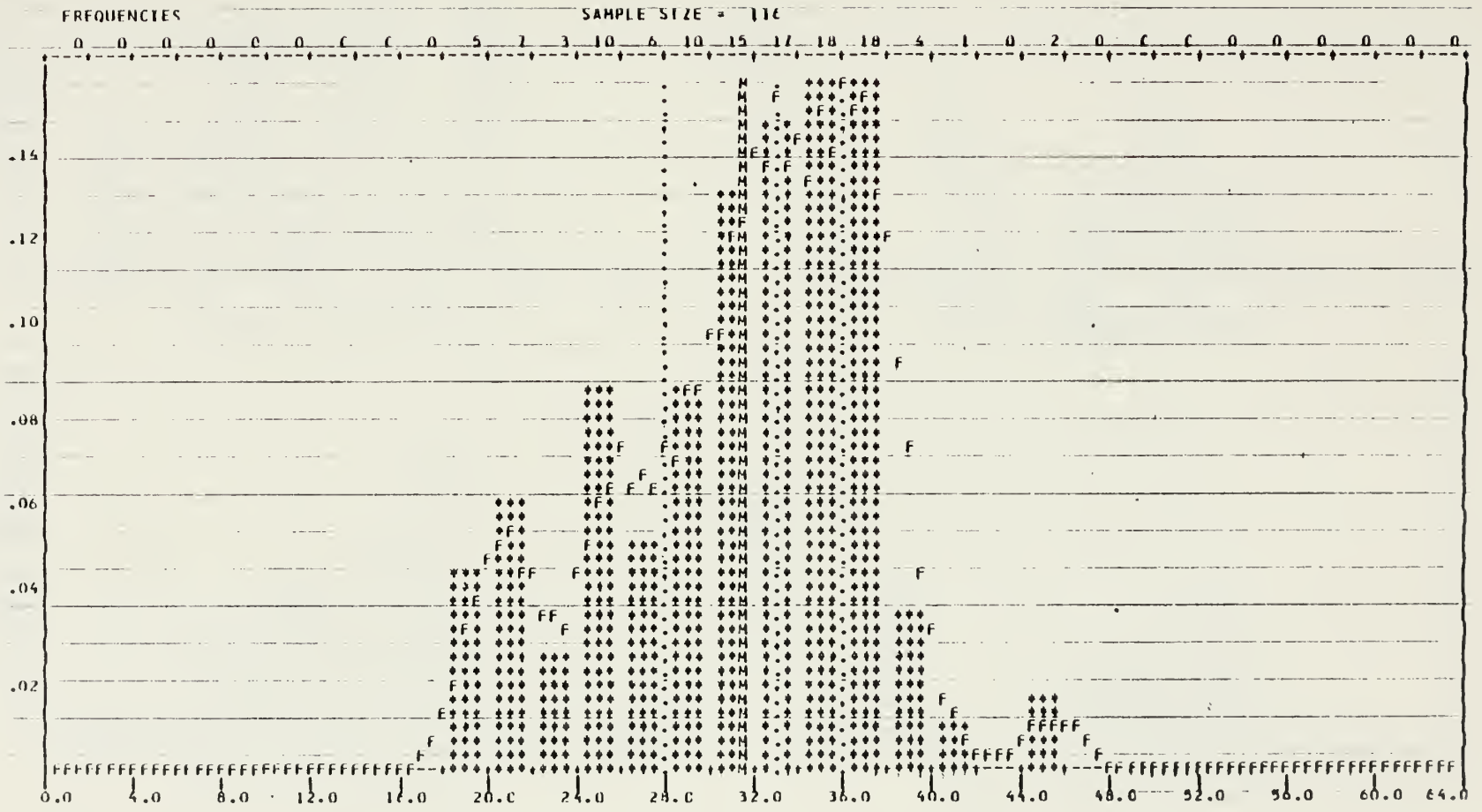

Figure 11. Frequency distribution of DMSP IR average digital count values (DCV's) for all fog duration categories (see Tables II and III); 30-60N, eastern North Pacific Ocean, 5-9 August 1976; (1) frequencies and sample size along abscissa (top), (2) percentage frequencies along ordinate, (3) M = mean DCV, (4) F = empirical density function.

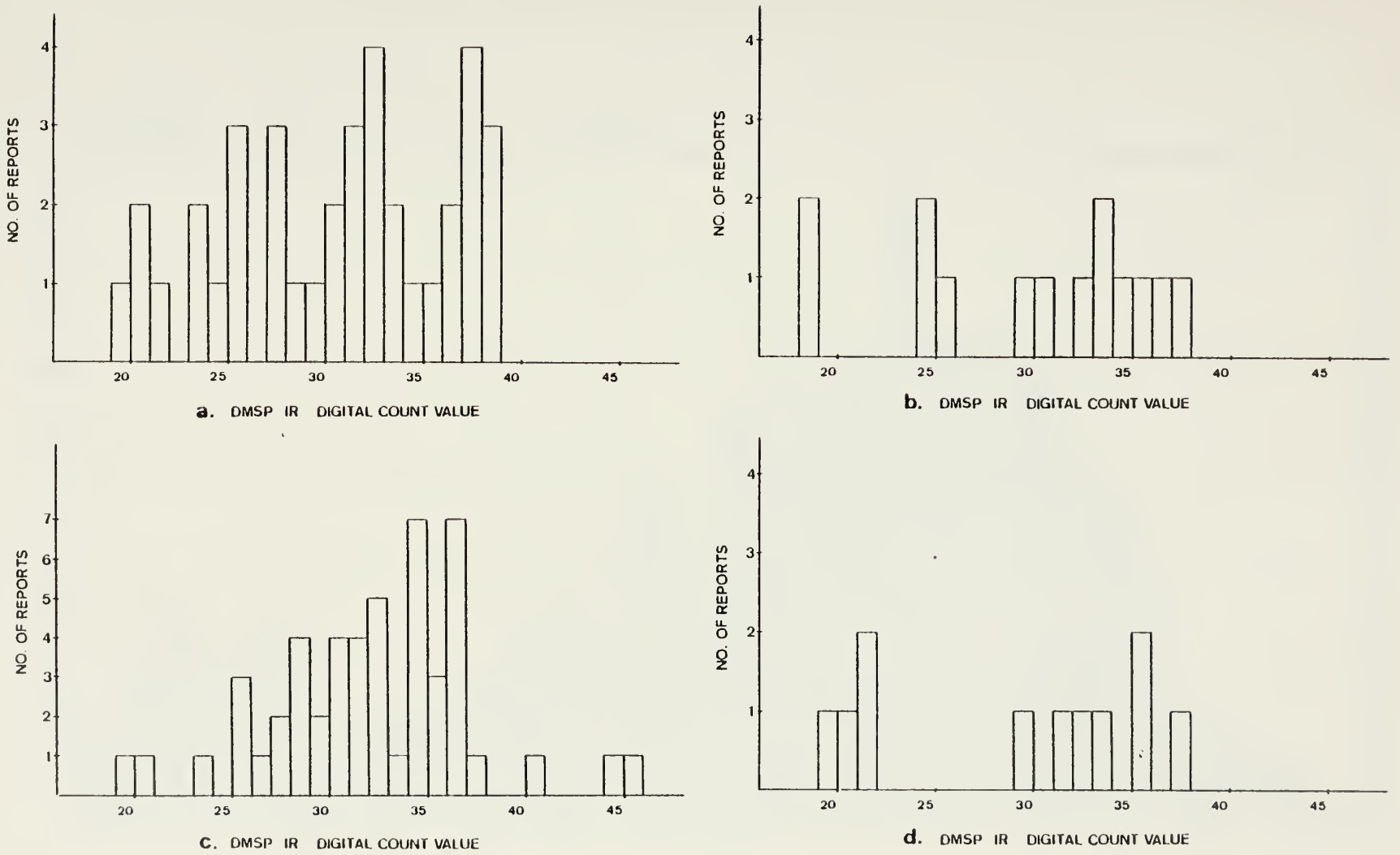

Figure 12. Frequency distribution of DMSP IR average count values for: (a) FDC GR 1; (b) FDC GR2 and FDC GR 3; (c) FDC 180; (d) FDC 175 (see Tables II and III); 30-60N, eastern North Pacific Ocean, 5-9 August 1976.

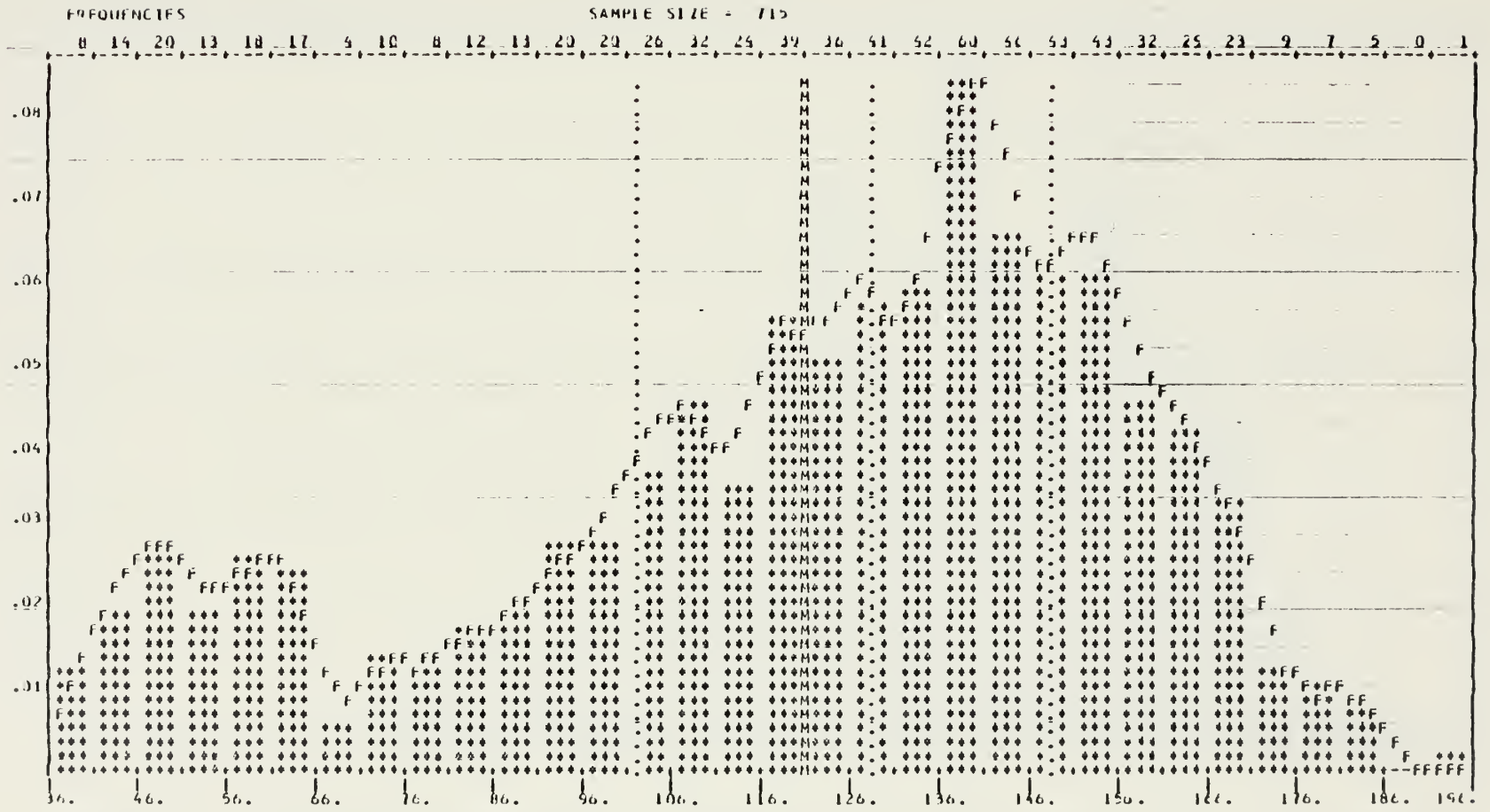

Figure 13. Frequency distribution of SMS-2 VIS average digital count values (DCV's) for all fog duration categories (see Tables II and III); 30-60N, eastern North Pacific Ocean, 5-9 August 1976; (1) frequencies and sample size along abscissa (top), (2) percentage frequencies along ordinate, (3) M = mean DCV, (4) F = empirical density function.

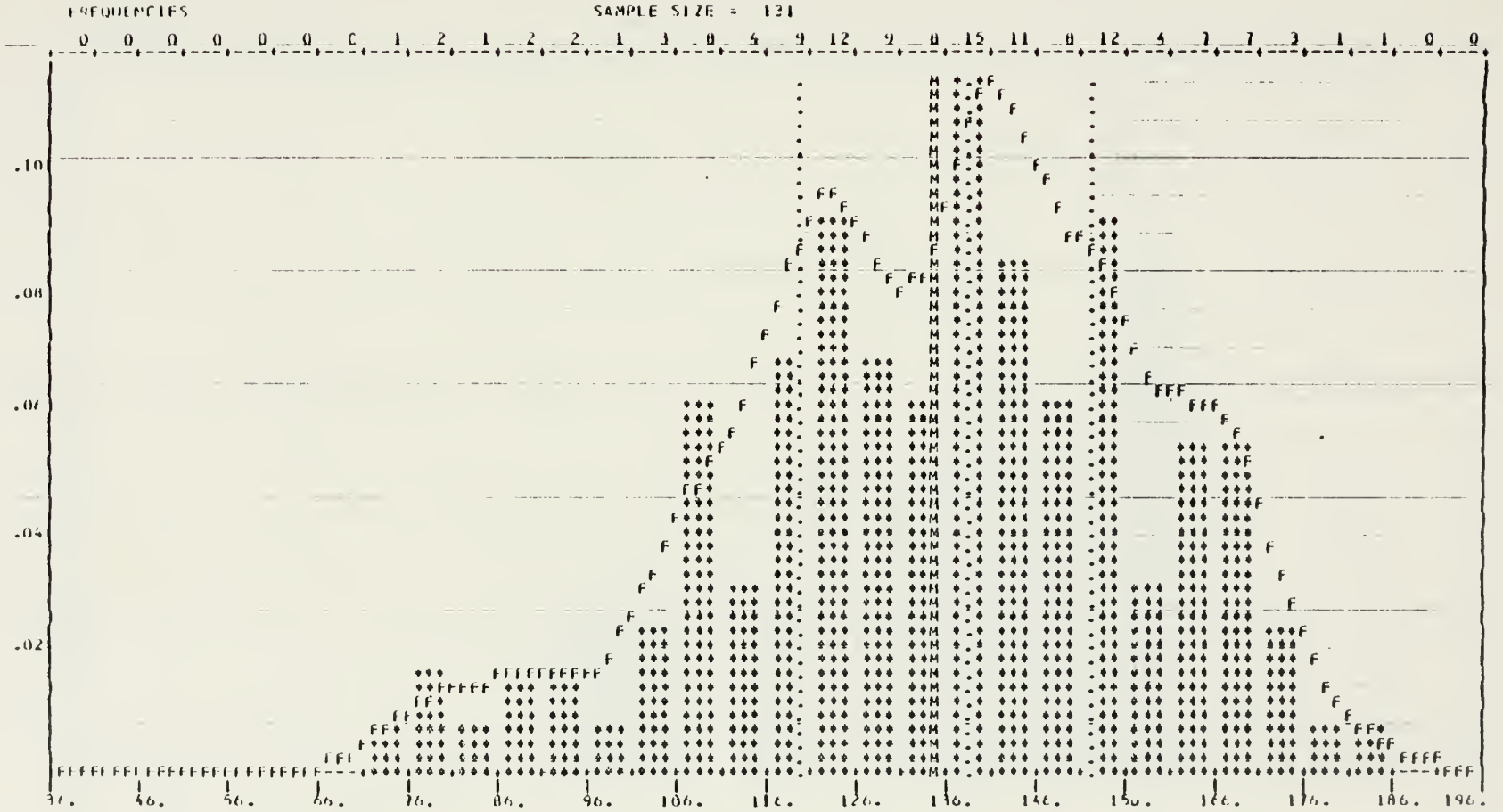

Figure 14. Frequency distribution of SMS-2 VIS average digital count values (DCV's) for fog duration category group 1 (see Tables II and III); 30-60N, eastern North Pacific Ocean, 5-9 August 1976; (1) frequencies and sample size along abscissa (top), (2) percentage frequencies along ordinate, (3) M = mean DCV, (4) F = empirical density function.

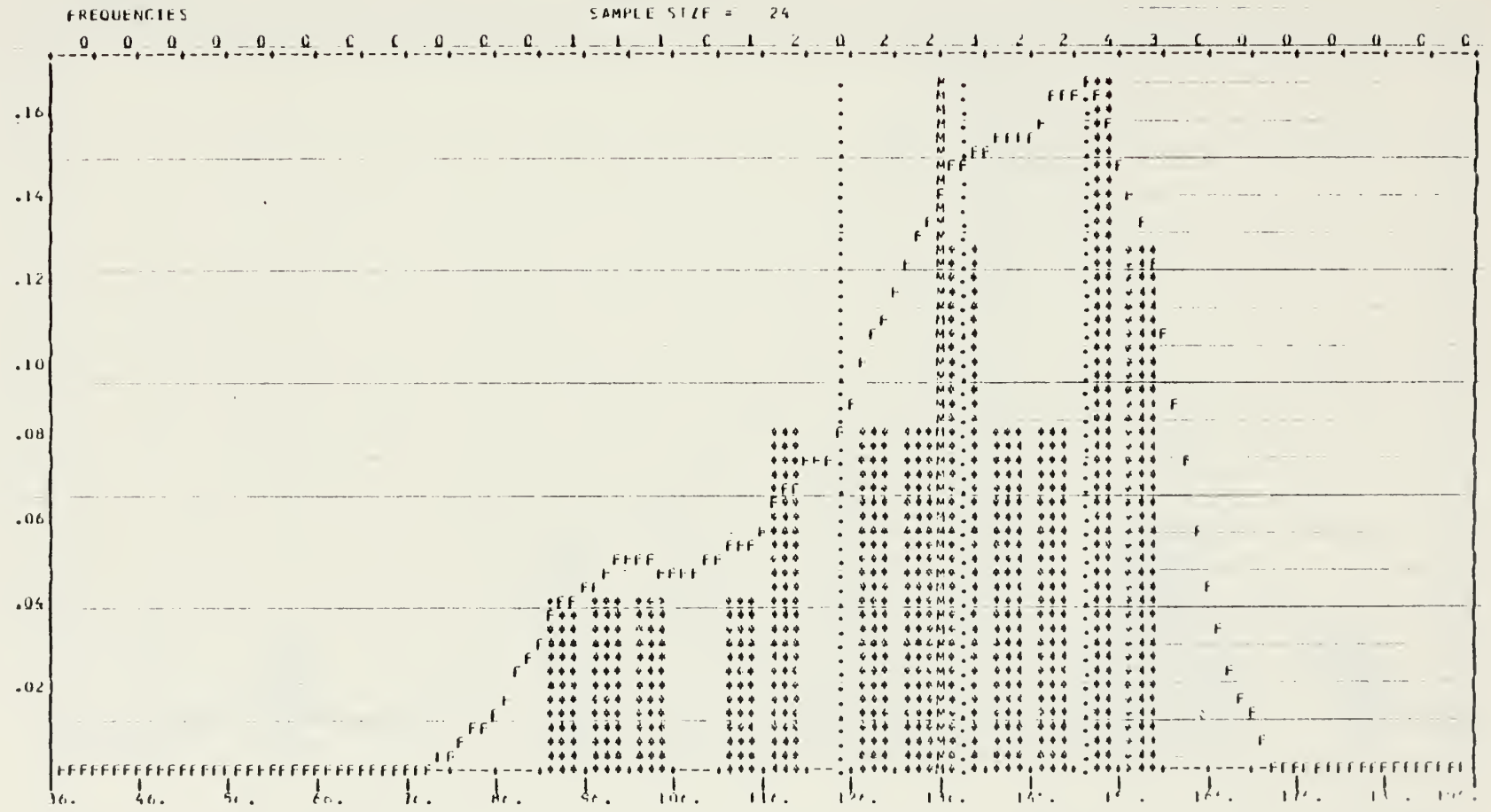

Figure 15. Frequency distribution of SMS-2 VIS average digital count values (DCV's) for fog duration category group 2 (see Tables II and III); 30-60N, eastern North Pacific Ocean, 5-9 August 1976; (1) frequencies and sample size along abscissa (top), (2) percentage frequencies along ordinate, (3) M = mean DCV, (4) F = empirical density function.

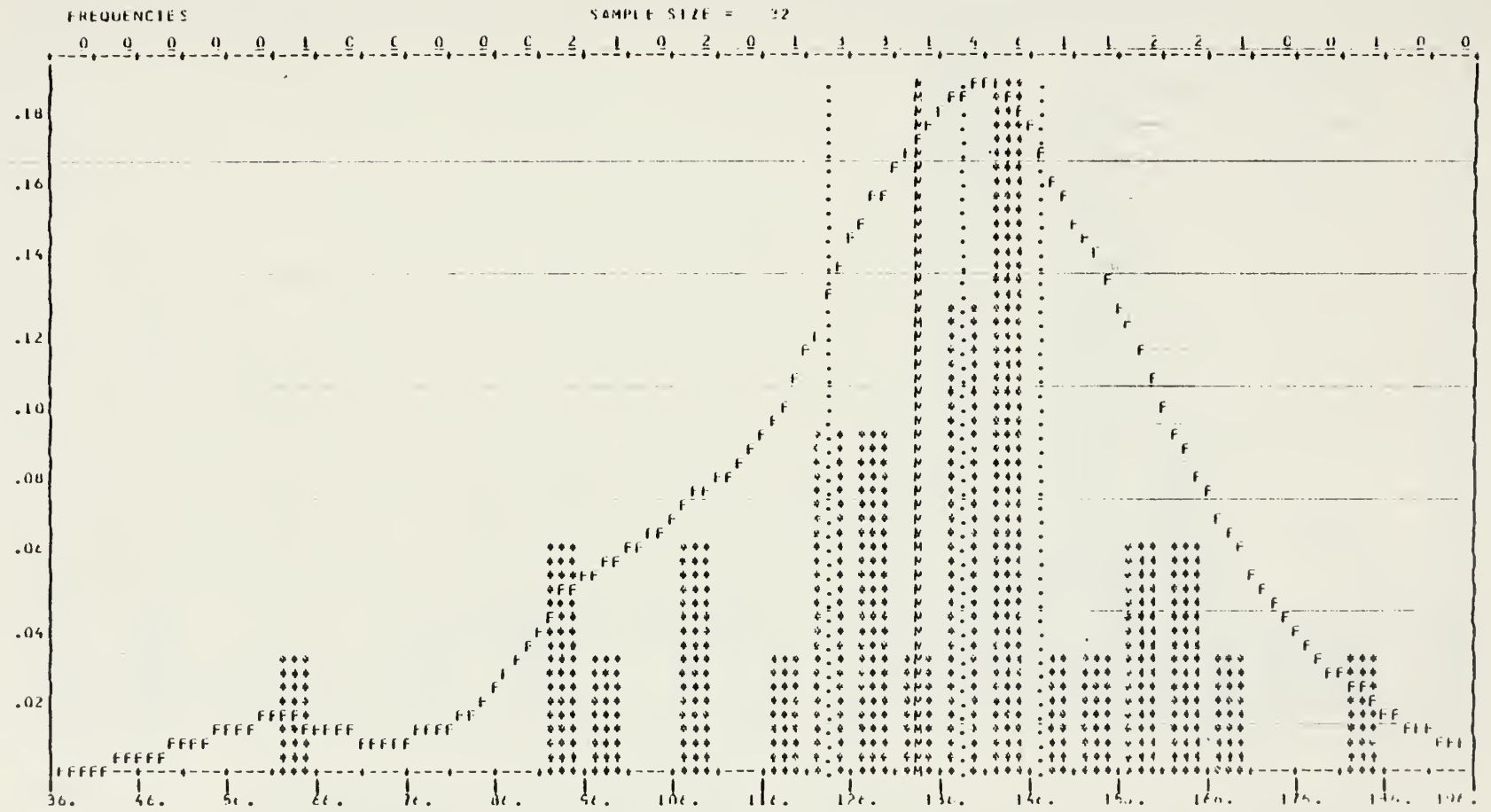

Figure 16. Frequency distribution of SMS-2 VIS average digital count values (DCV's) for fog duration category group 3 (see Tables II and III); 30-60N, eastern North Pacific Ocean, 5-9 August 1976; (1) frequencies and sample size along abscissa (top), (2) percentage frequencies along ordinate, (3) M = mean DCV, (4) F = empirical density function.

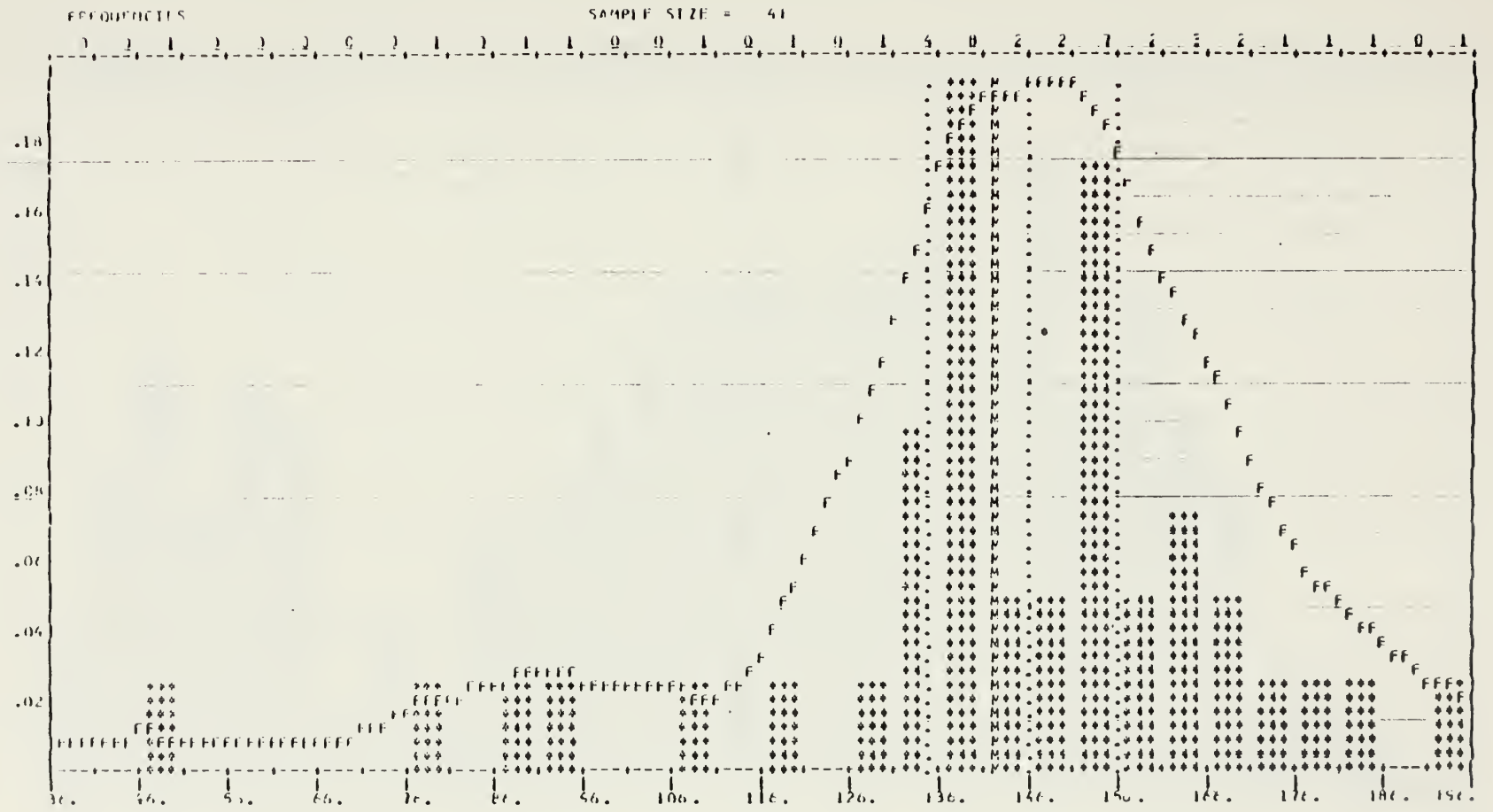

Figure 17. Frequency distribution of SMS-2 VIS average digital count values (DCV's) for fog duration category 175 (see Tables II and III); 30-60N, eastern North Pacific Ocean, 5-9 August 1976; (1) frequencies and sample size along abscissa (top), (2) percentage frequencies along ordinate, (3) M = mean DCV, (4) F = empirical density function.

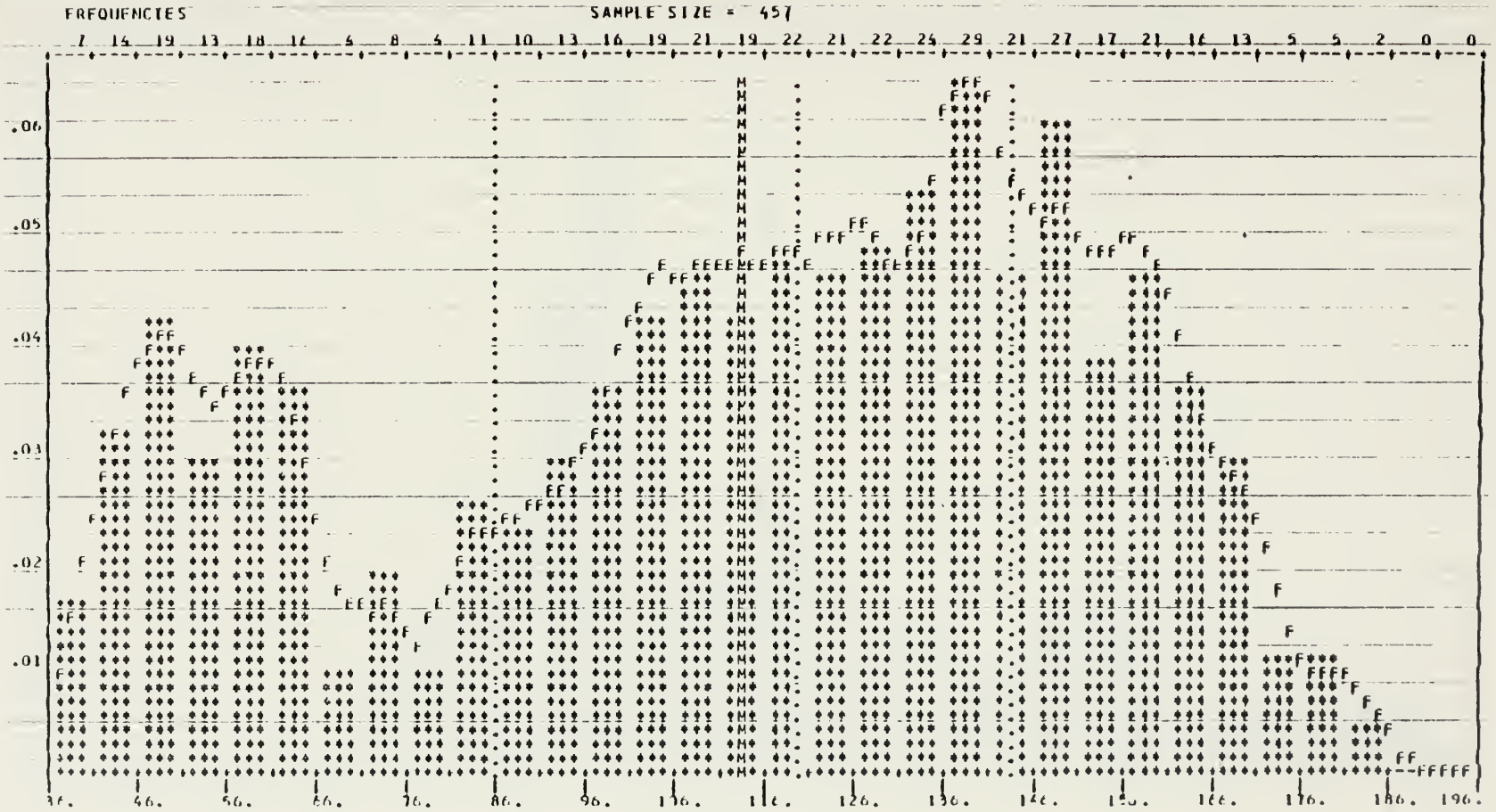

Figure 18. Frequency distribution of SMS-2 VIS average digital count values (DCV's) for fog duration category 180 (see Tables II and III); 30-60N, eastern North Pacific Ocean, 5-9 August 1976; (1) frequencies and sample size along abscissa (top), (2) percentage frequencies along ordinate, (3) M = mean DCV, (4) F = empirical density function.

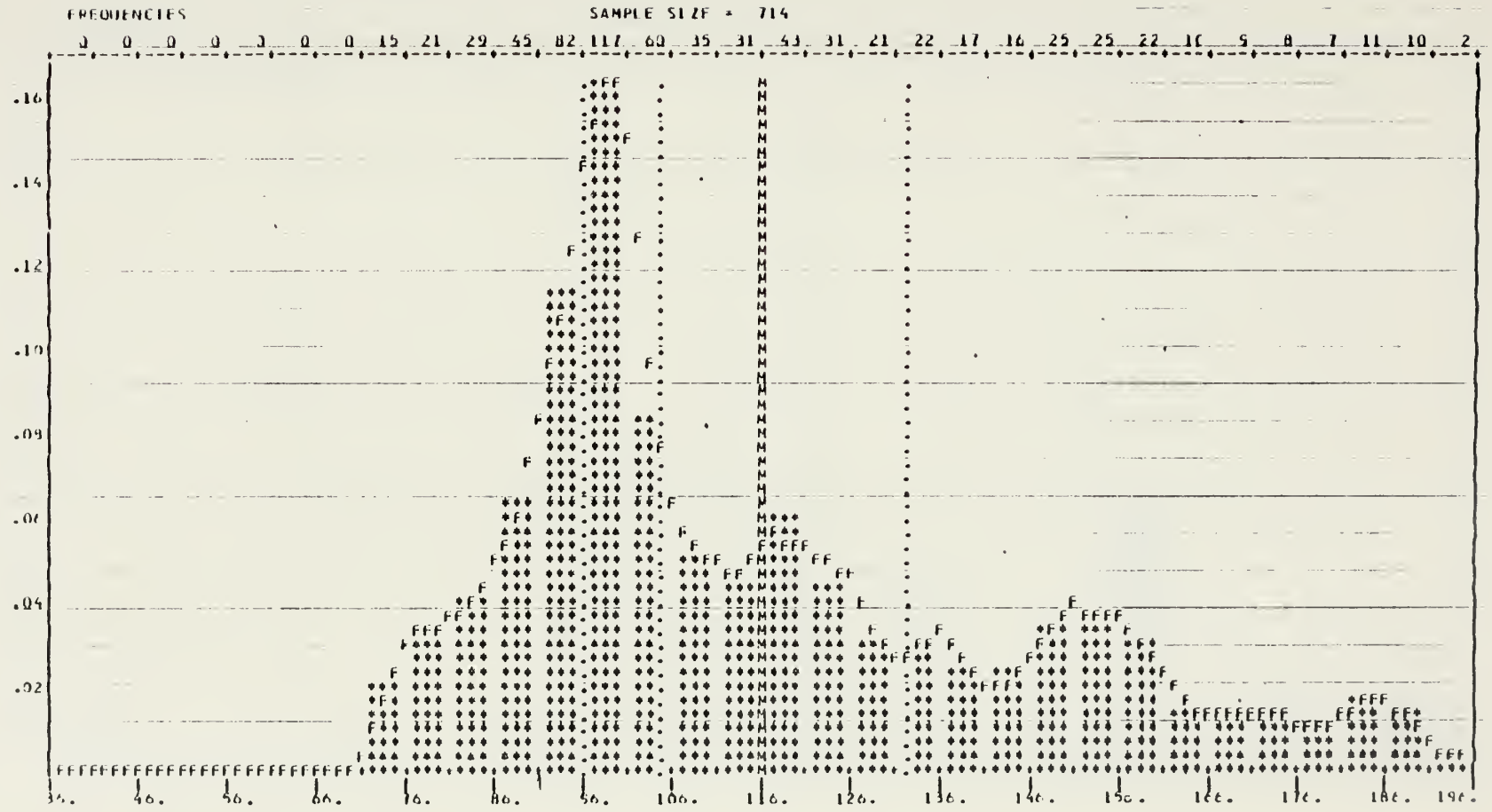

Figure 19. Frequency distribution of SMS-2 IR average digital count values (DCV's) for all fog duration categories (see Tables II and III); 30-60N, eastern North Pacific Ocean, 5-9 August 1976; (1) frequencies and sample size along abscissa (top), (2) percentage frequencies along ordinate, (3) M = mean DCV, (4) F = empirical density function.

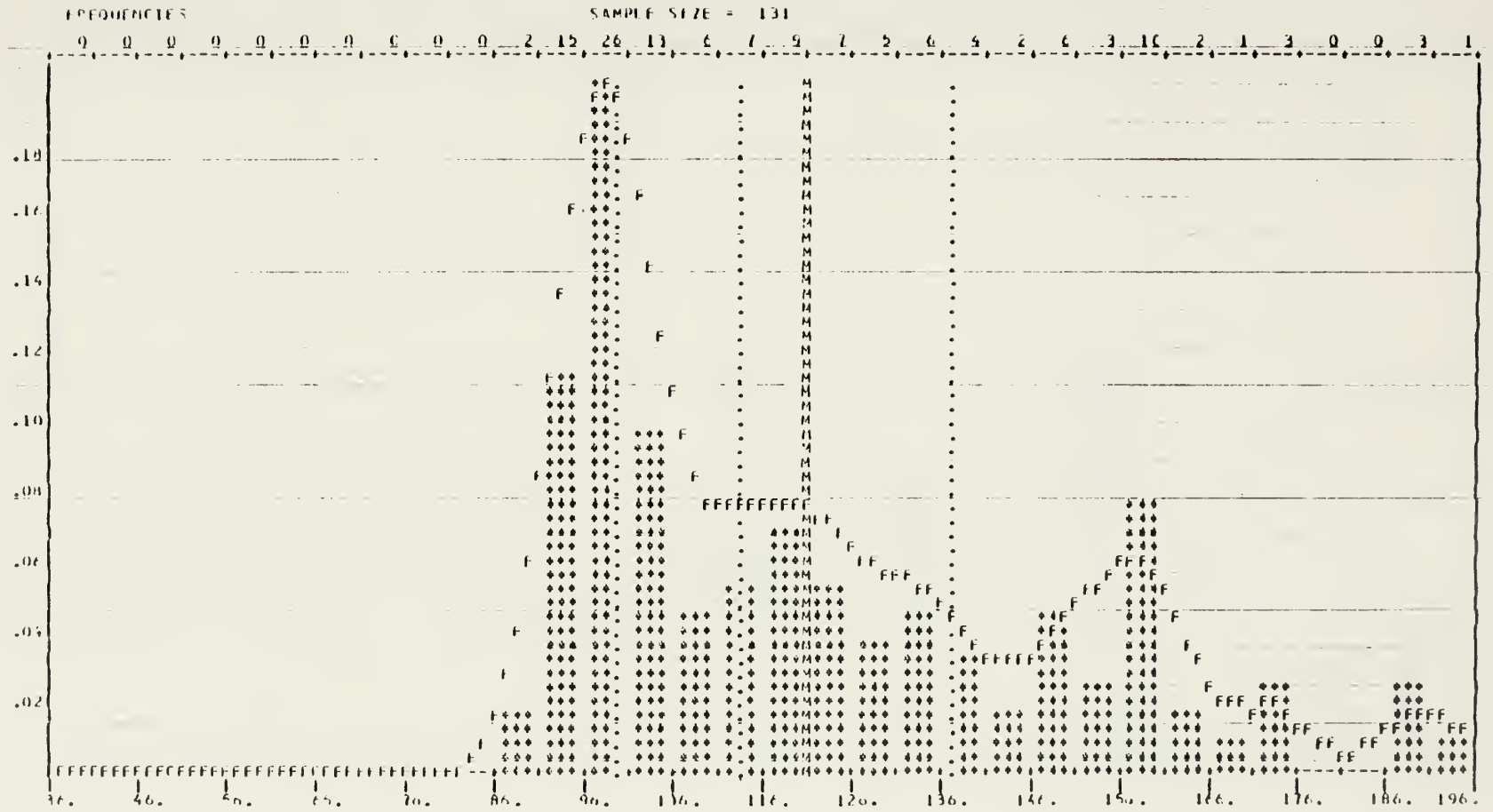

Figure 20. Frequency distribution of SMS-2 IR average digital count values (DCV's) for fog duration category group 1 (see Tables II and III); 30-60N, eastern North Pacific Ocean, 5-9 August 1976; (1) frequencies and sample size along abscissa (top), (2) percentage frequencies along ordinate, (3) M = mean DCV, (4) F = empirical density function.

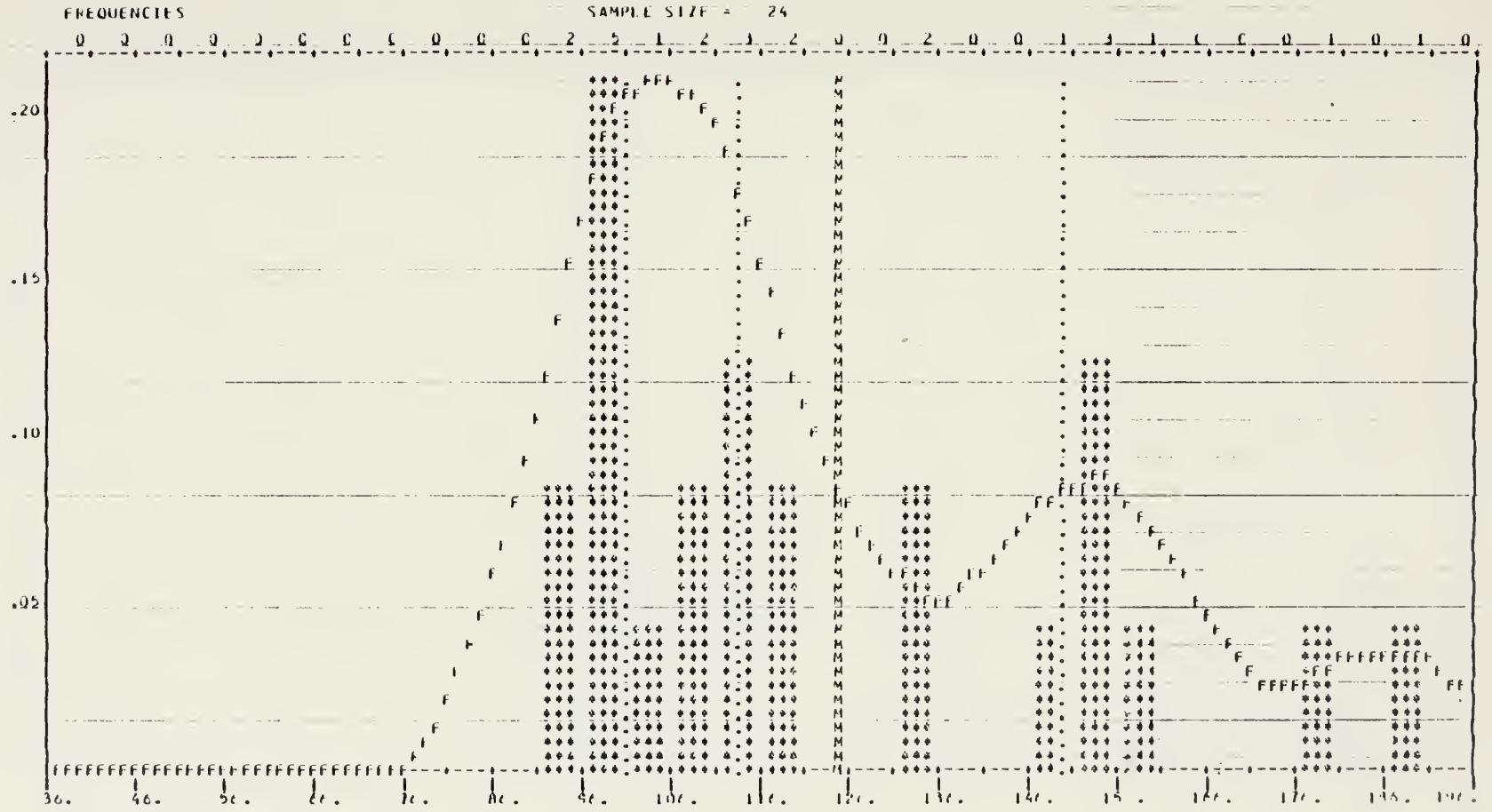

Figure 21. Frequency distribution of SMS-2 IR average digital count values (DCV's) for fog duration category group 2 (see Tables II and III); 30-60N, eastern North Pacific Ocean, 5-9 August 1976; (1) frequencies and sample size along abscissa (top), (2) percentage frequencies along ordinate, (3) M = mean DCV, (4) F = empirical density function.

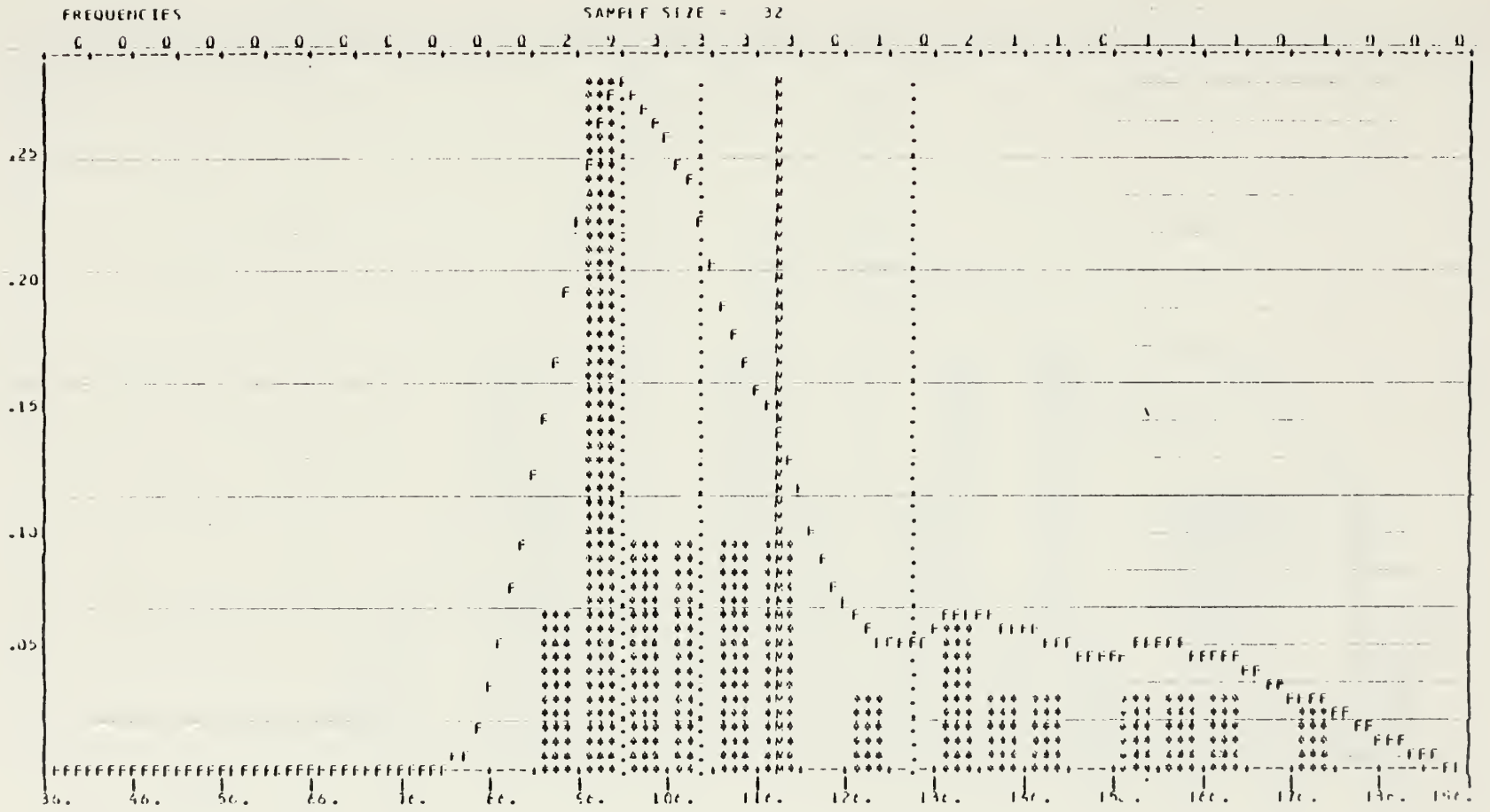

Figure 22. Frequency distribution of SMS-2 IR average digital count values (DCV's) for fog duration category group 3 (see Tables II and III); 30-60N, eastern North Pacific Ocean, 5-9 August 1976; (1) frequencies and sample size along abscissa (top), (2) percentage frequencies along ordinate, (3) M = mean DCV, (4) F = empirical density function.

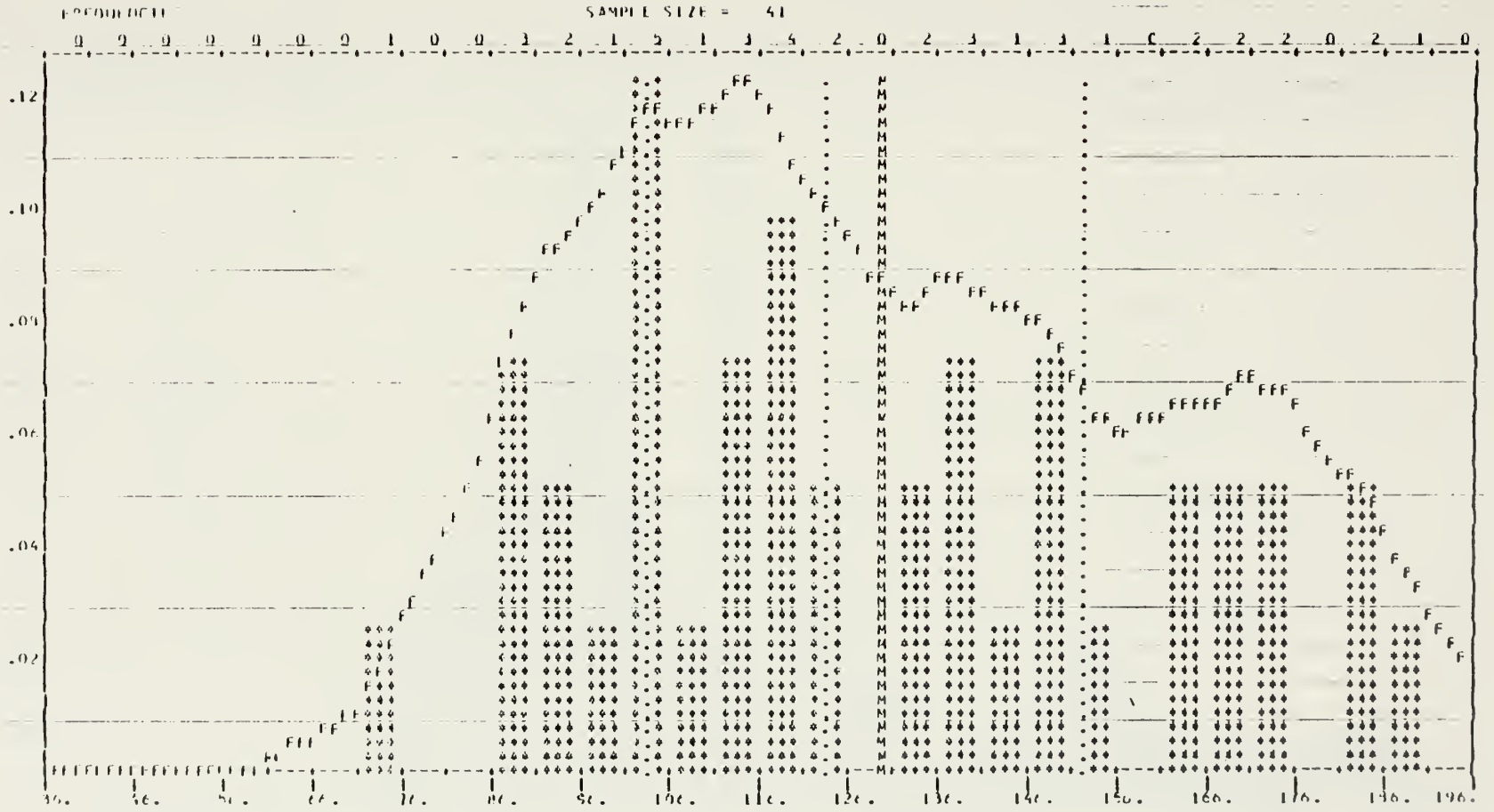

Figure 23. Frequency distribution of SMS-2 IR average digital count values (DCV's) for fog duration category 175 (see Tables II and III); 30-60N, eastern North Pacific Ocean, 5-9 August 1976; (1) frequencies and sample size along abscissa (top), (2) percentage frequencies along ordinate, (3) M = mean DCV, (4) F = empirical density function.

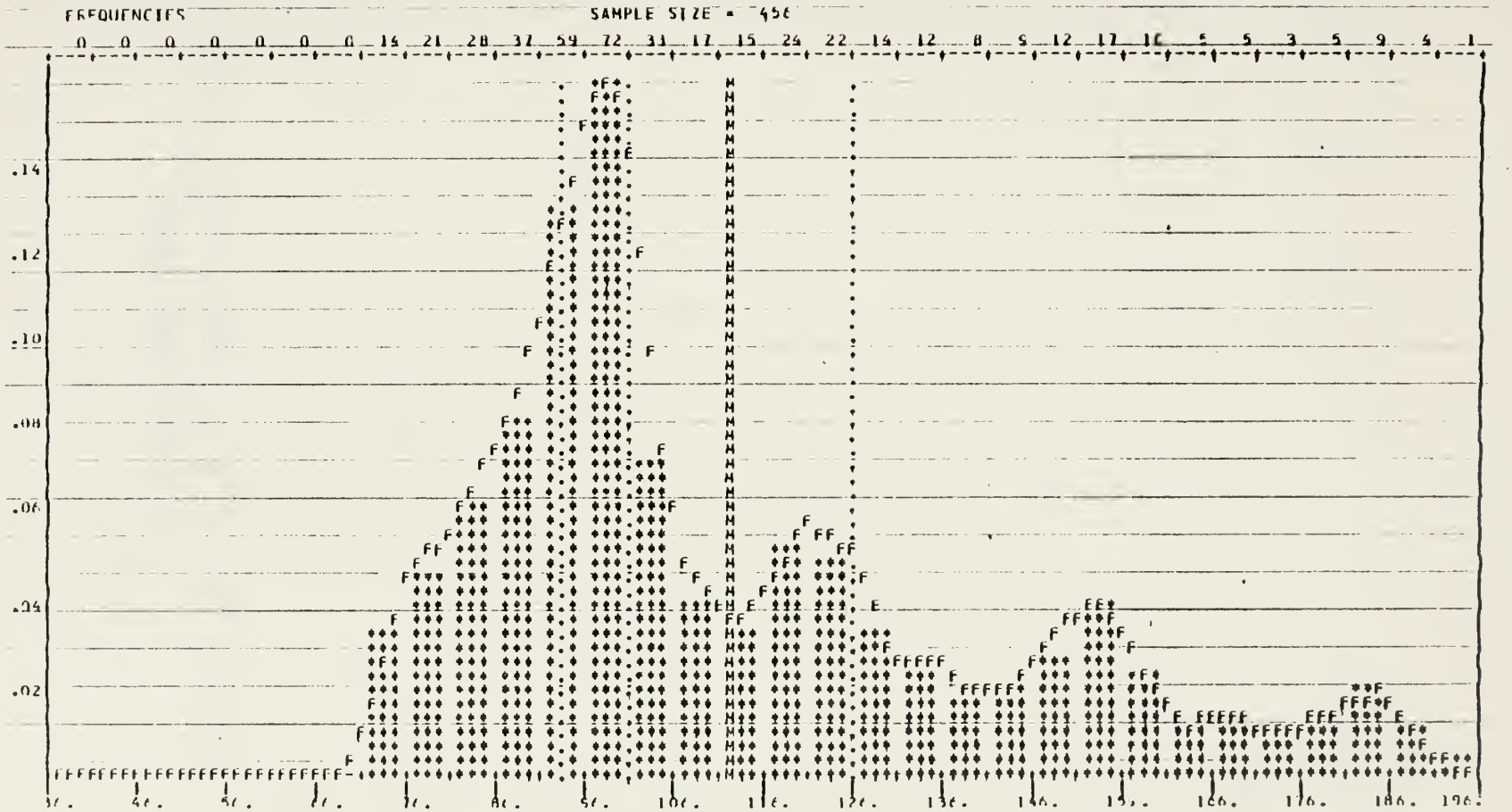

Figure 24. Frequency distribution of SMS-2 IR average digital count values (DCV's) for fog duration category 180 (see Tables II and III); 30-60N, eastern North Pacific Ocean, 5-9 August 1976; (1) frequencies and sample size along abscissa (top), (2) percentage frequencies along ordinate, (3) M = mean DCV, (4) F = empirical density function.

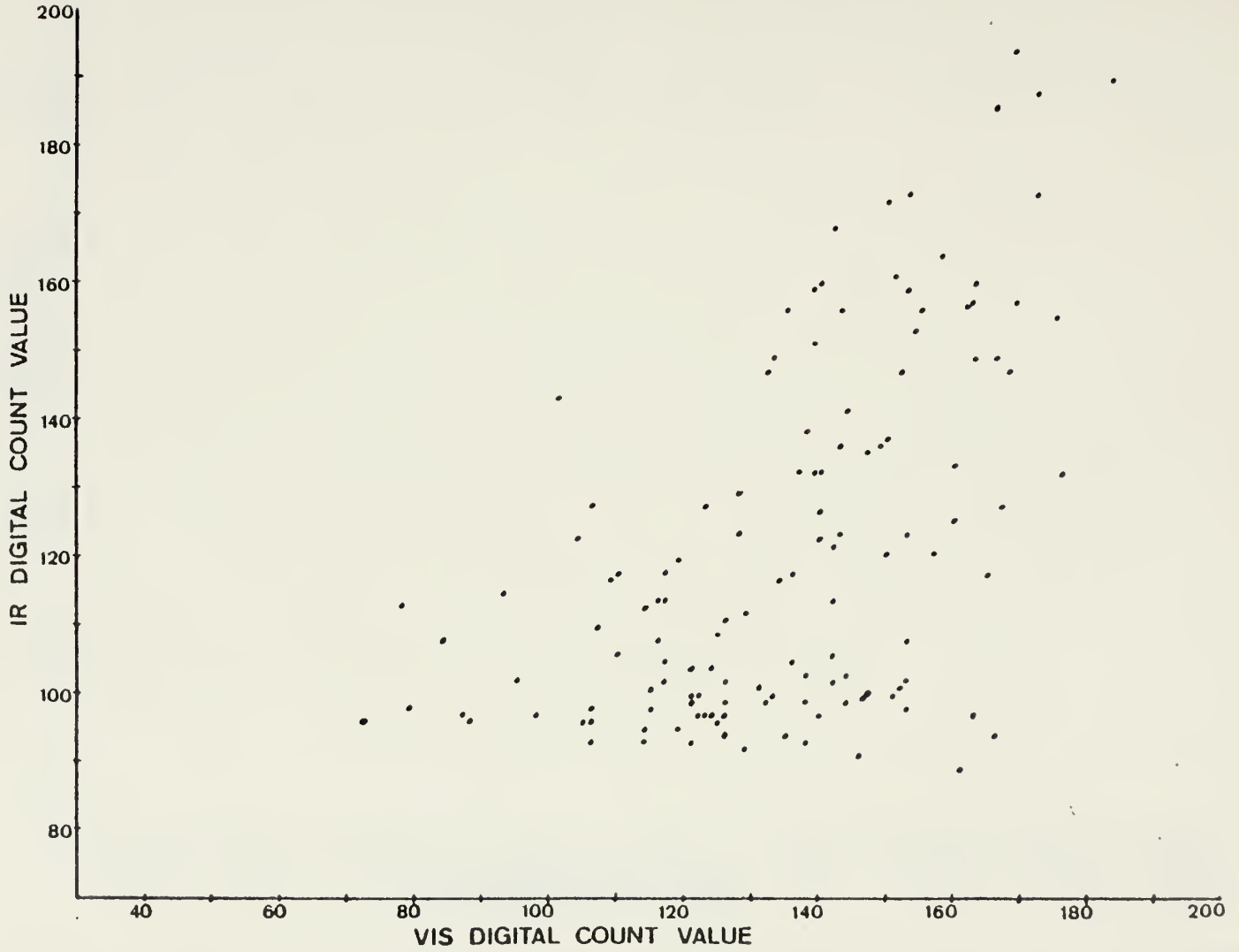

Figure 25. Scatter diagram of SMS-2 VIS vs. IR average digital count values (DCV's) for fog duration category group 1 (see Tables II and III); 30-60N, eastern North Pacific Ocean, 5-9 August 1976.

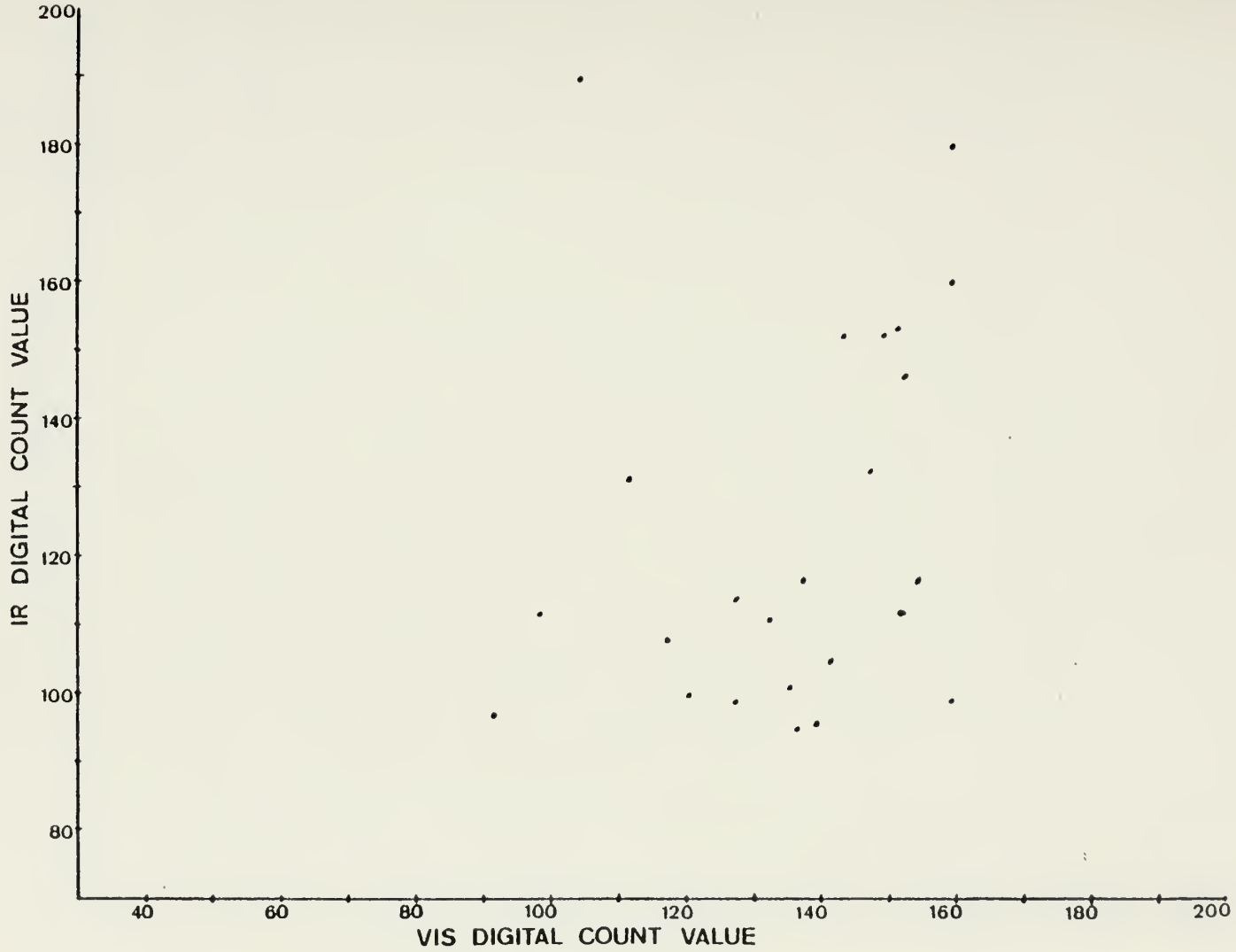

Figure 26. Scatter diagram of SMS-2 VIS vs. IR average digital count values (DCV's) for fog duration category group 2 (see Tables II and III); 30-60N, eastern North Pacific Ocean, 5-9 August 1976.

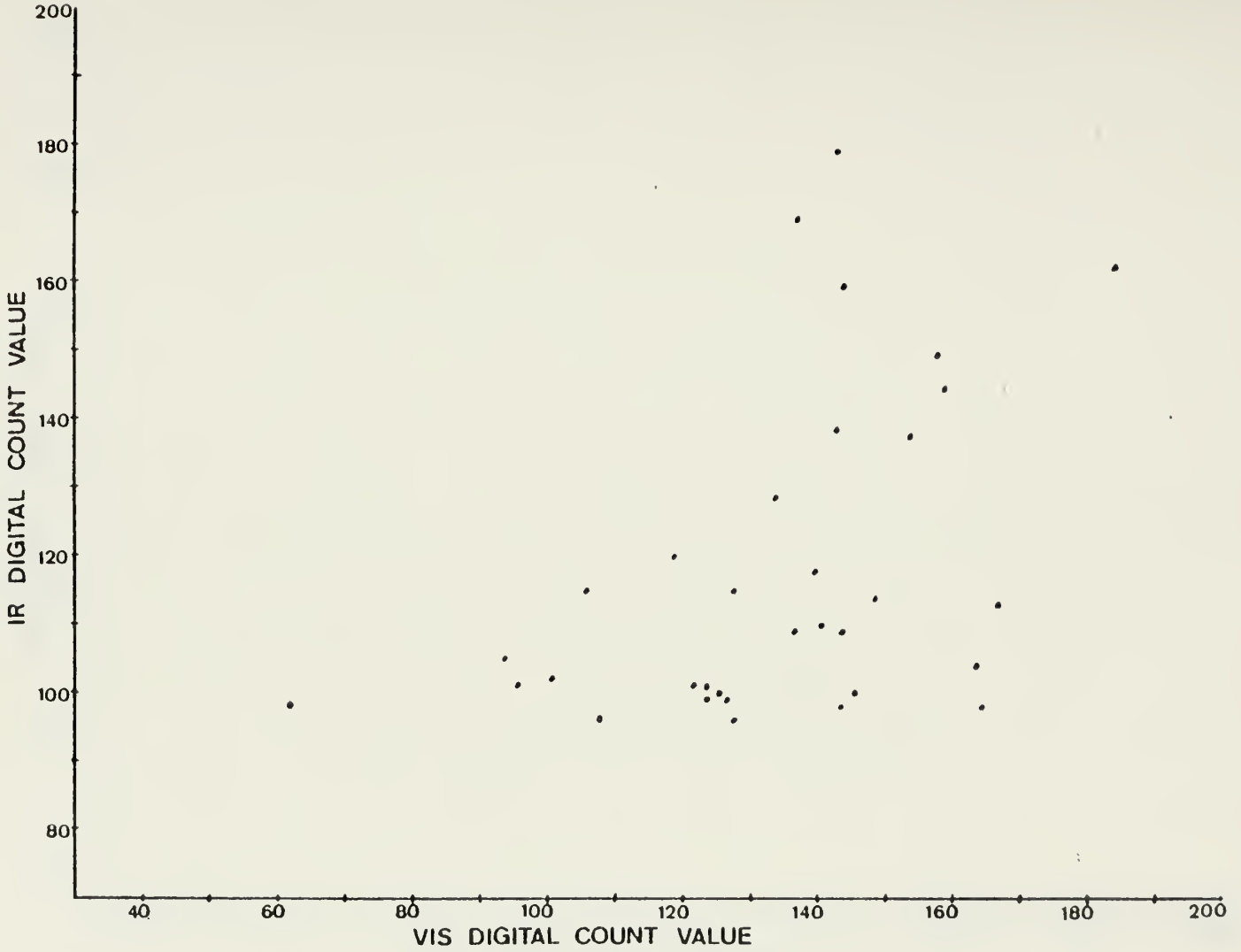

Figure 27. Scatter diagram of SMS-2 VIS vs. IR average digital count values (DCV's) for fog duration category group 3 (see Tables II and III); 30-60N, eastern North Pacific Ocean, 5-9 August 1976.

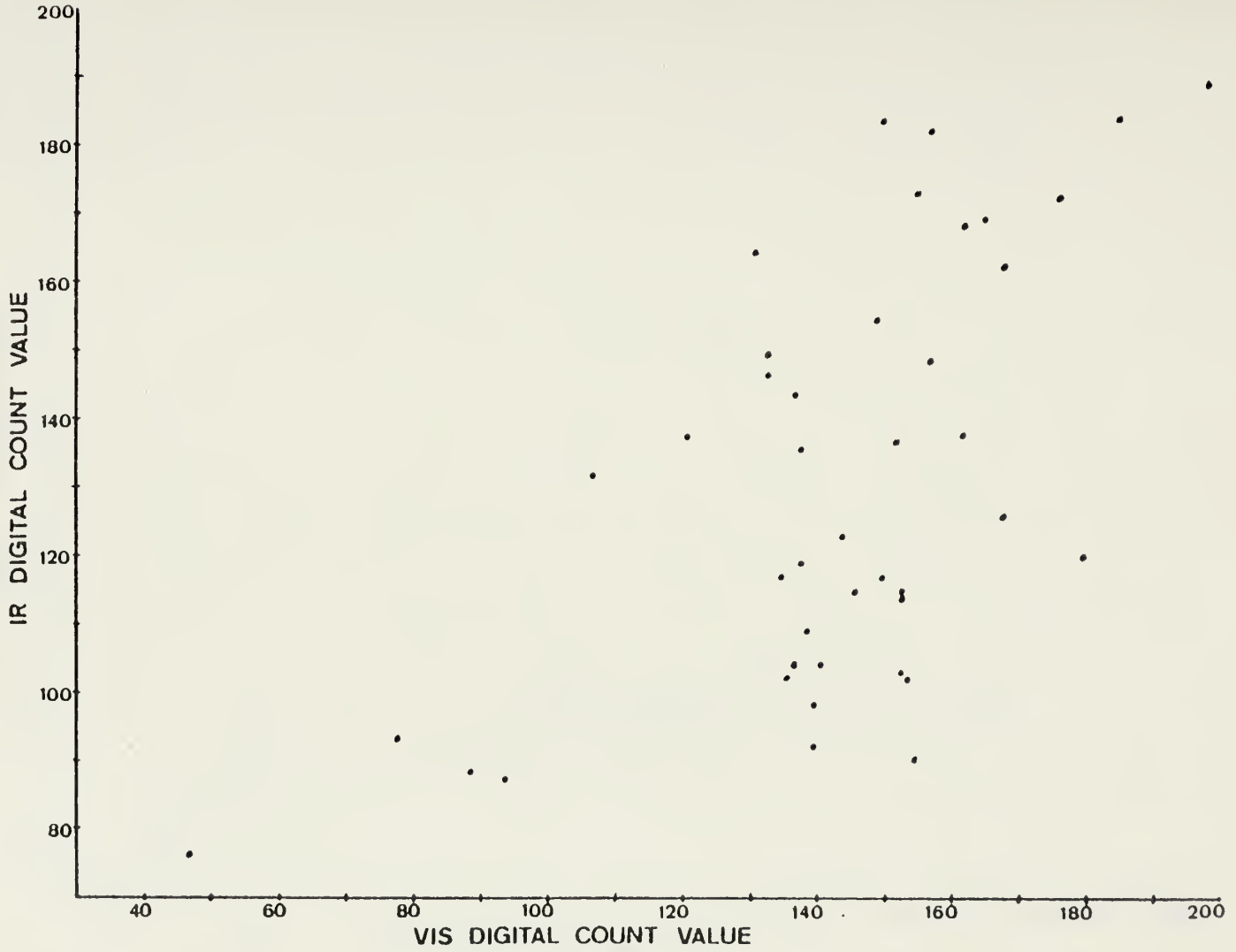

Figure 28. Scatter diagram of SMS-2 VIS vs. IR average digital count values (DCV's) for fog duration category 175 (see Tables II and III); 30-60N, eastern North Pacific Ocean, 5-9 August 1976.

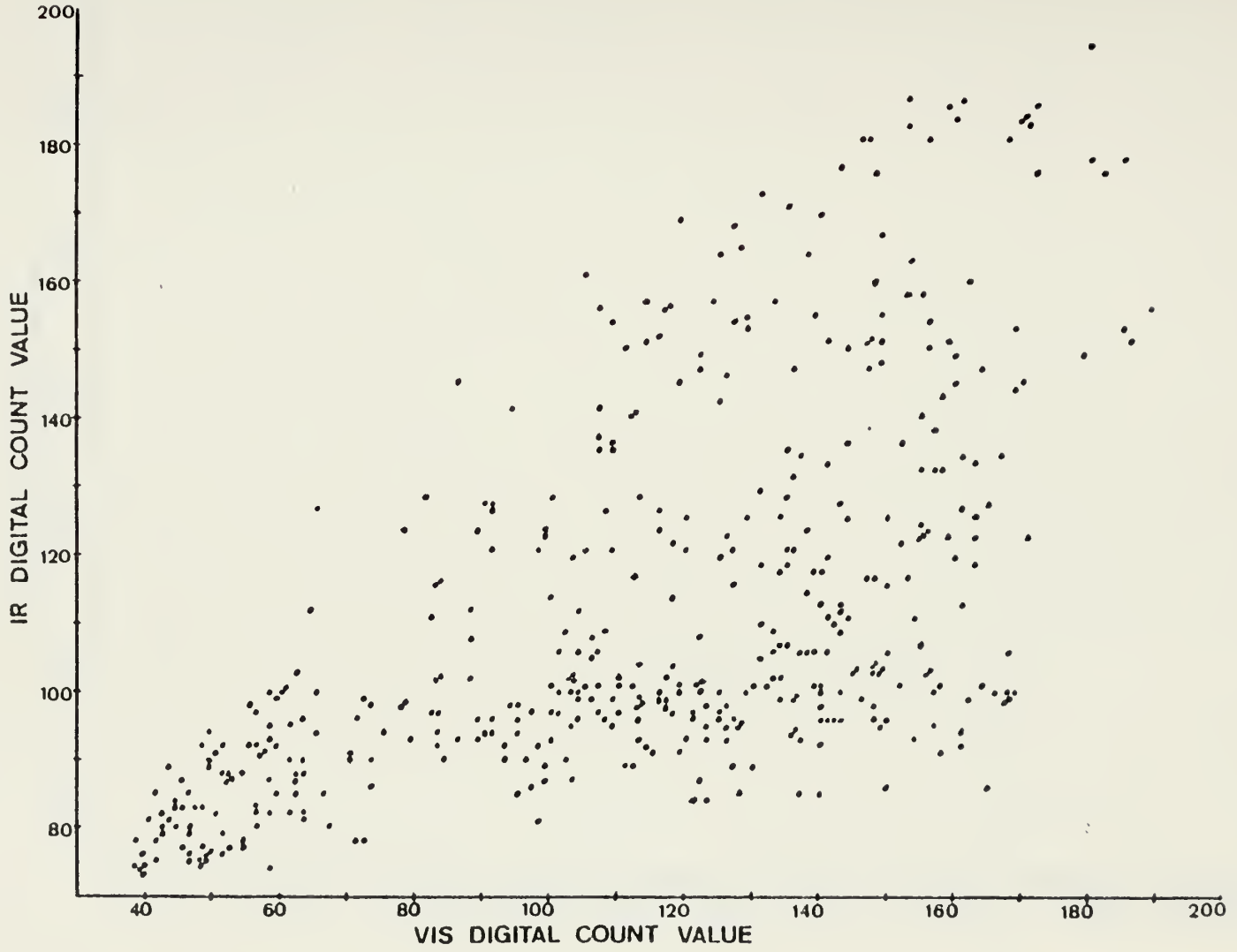

Figure 29. Scatter diagram of SMS-2 VIS vs. IR average digital count values (DCV's) for fog duration category 180 (see Tables II and III); 30-60N, eastern North Pacific Ocean, 5-9 August 1976.

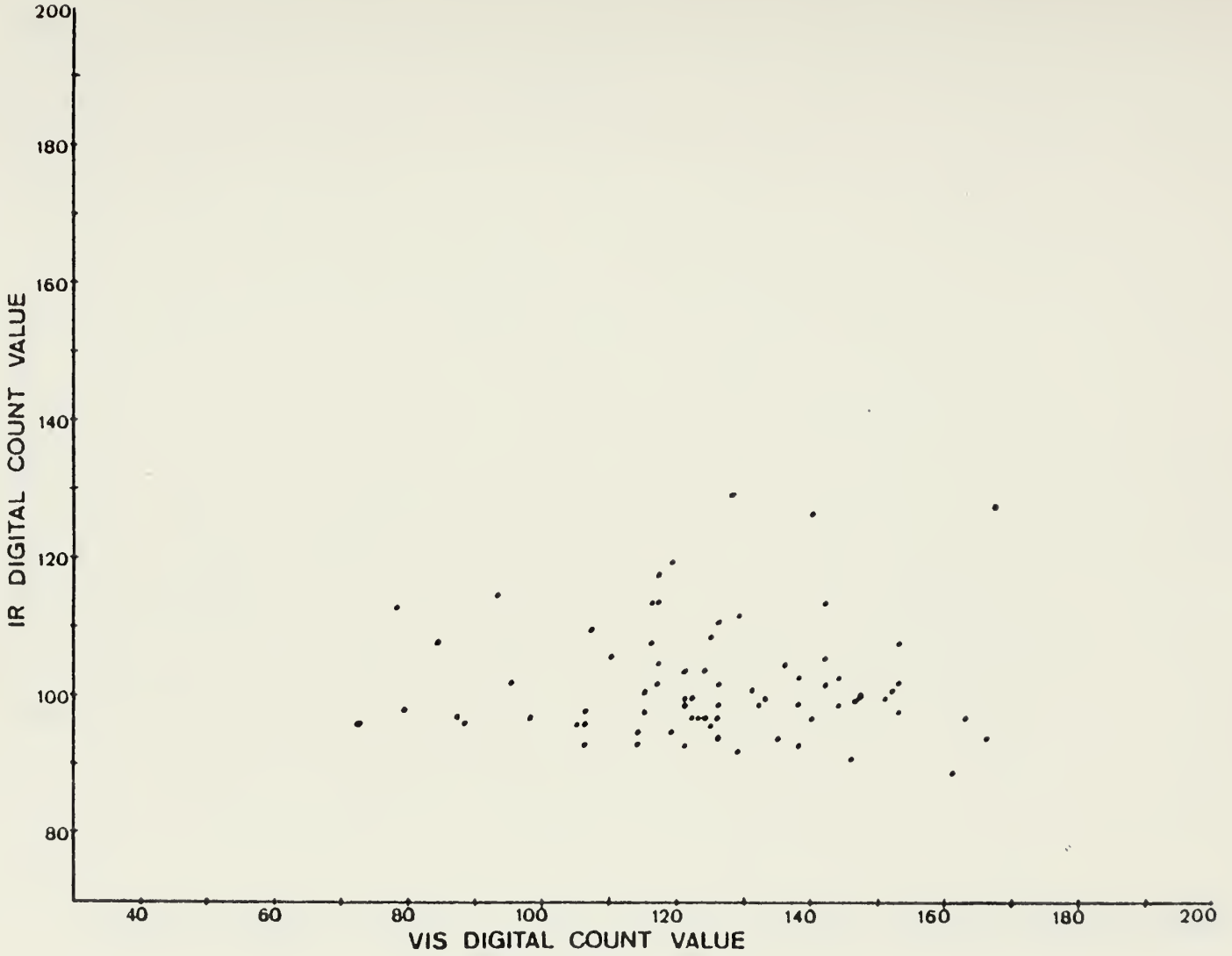

Figure 30. Scatter diagram of SMS-2 VIS vs. IR average digital count values (DCV's) for fog duration category group 1 (see Tables II and III); middle and/or high cloud cases removed; 30-60N, eastern North Pacific Ocean, 5-9 August 1976.

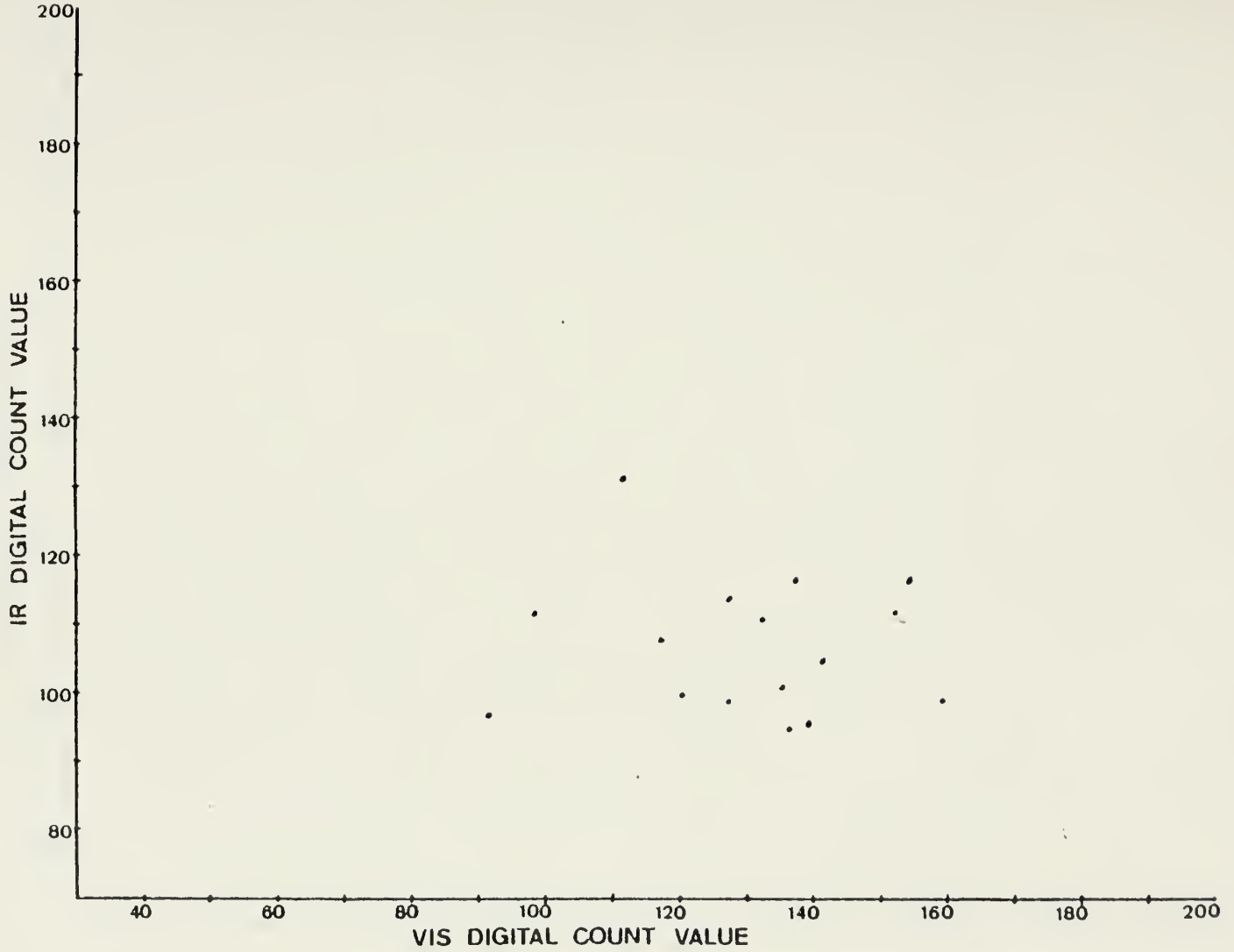

Figure 31. Scatter diagram of SMS-2 VIS vs. IR average digital count values (DCV's) for fog duration category group 2 (see Tables II and III); middle and/or high cloud cases removed; 30-60N, eastern North Pacific Ocean, 5-9 August 1976.

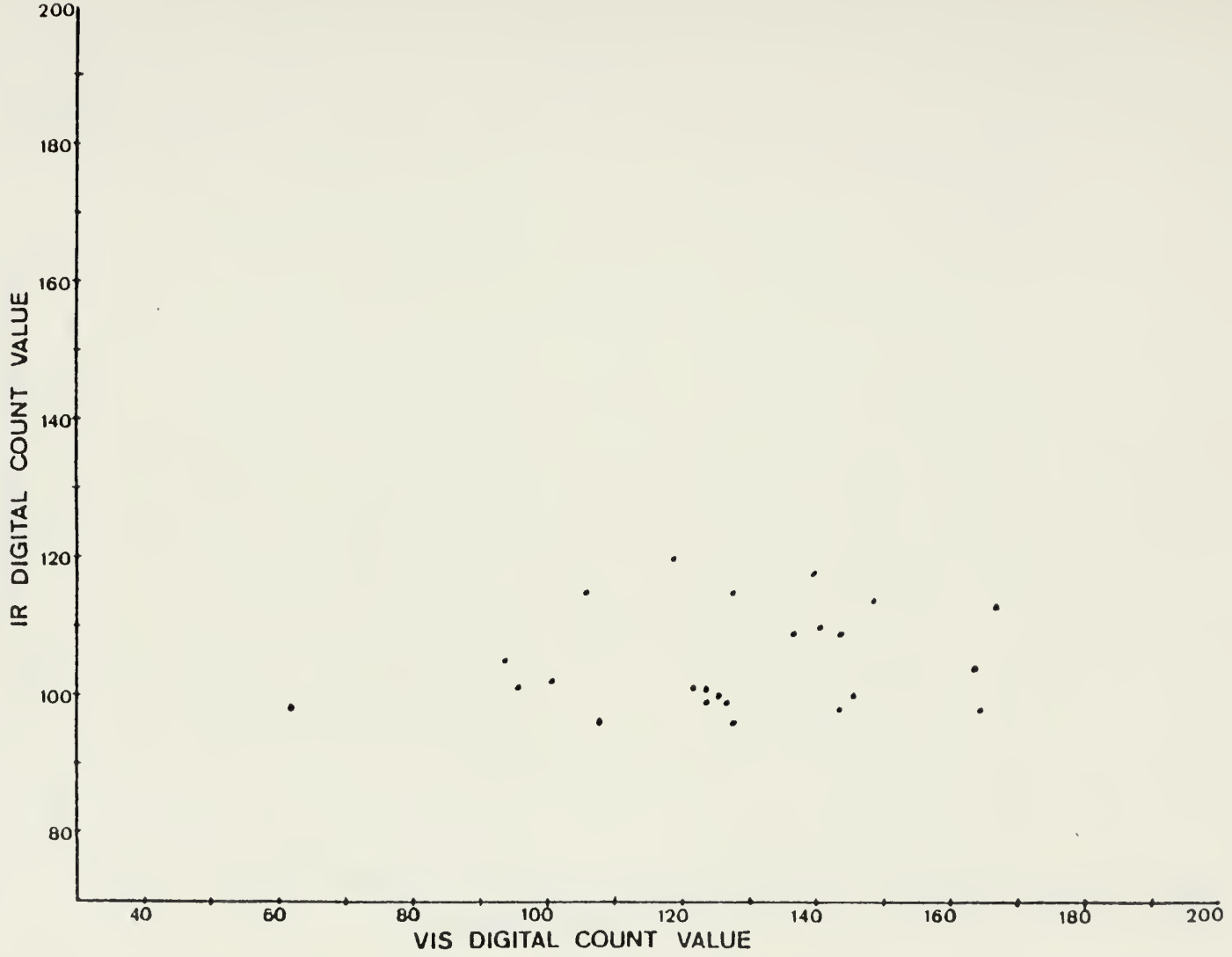

Figure 32. Scatter diagram of SMS-2 VIS vs. IR average digital count values (DCV's) for fog duration category group 3 (see Tables II and III); middle and/or high cloud cases removed; 30-60N, eastern North Pacific Ocean, 5-9 August 1976.

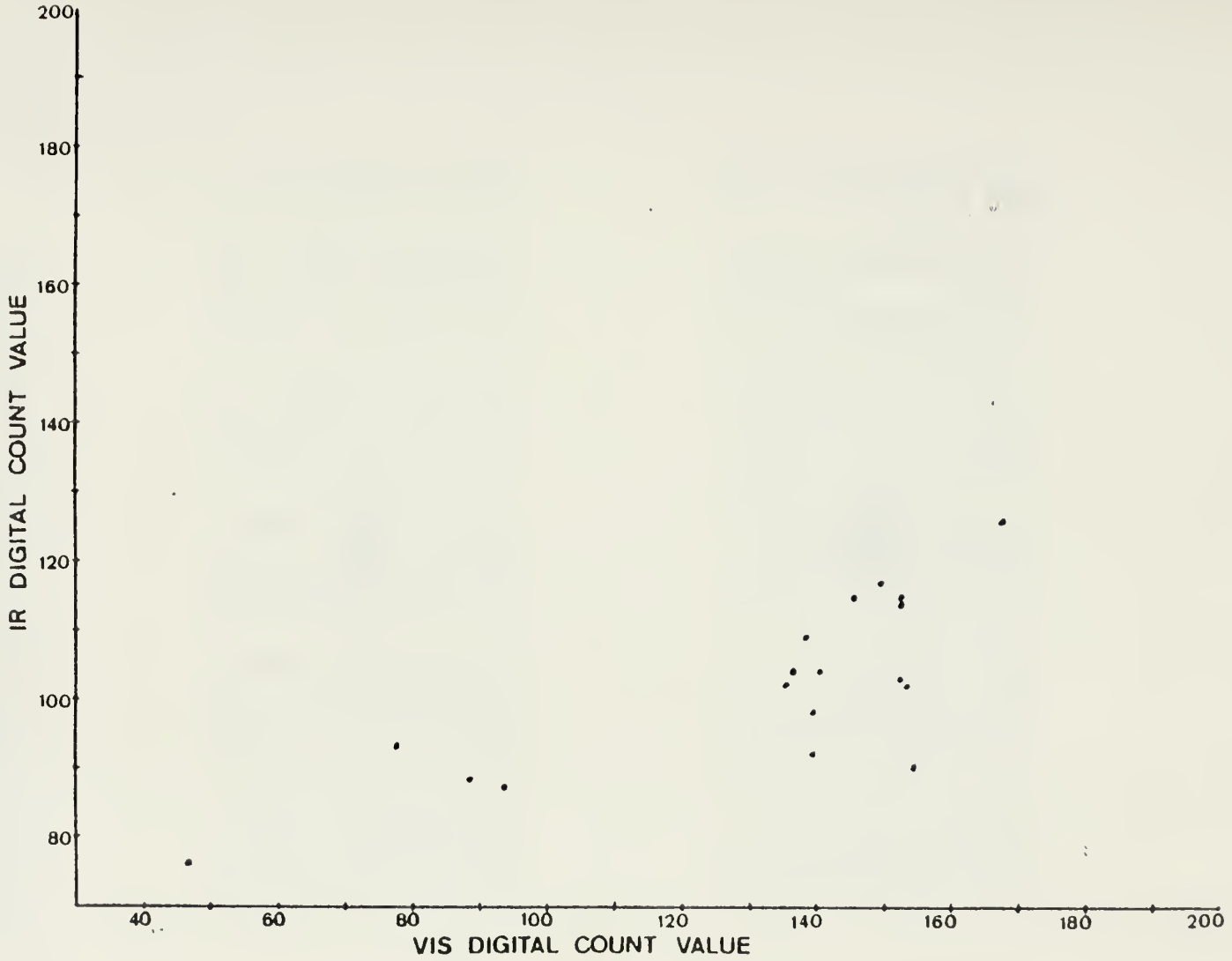

Figure 33. Scatter diagram of SMS-2 VIS vs. IR average digital count values (DCV's) for fog duration category 175 (see Tables II and III); middle and/or high cloud cases removed; 30-60N, eastern North Pacific Ocean, 5-9 August 1976.

100	95	91	82	93	103	119	109	79	76	99
108	107	111	84	87	82	101	77	66	65	72
111	118	122	114	119	129	126	89	66	63	94
125	129	133	125	119	121	130	132	100	75	103
135	141	129	110	123	140	141	144	128	134	120
132	115	120	131	118	(122)	136	112	114	131	117
146	116	137	126	134	140	145	113	88	91	91
140	139	137	115	152	140	128	97	86	102	158
141	150	125	120	118	125	82	74	69	91	161
135	137	149	99	126	94	65	72	71	86	135
149	157	169	173	145	87	74	70	69	86	83

104	101	102	101	101	101	97	99	103	107	117
104	101	102	101	101	101	97	99	103	107	117
103	103	103	102	100	97	98	102	117	136	152
103	103	103	102	100	97	98	102	117	136	152
101	101	101	101	101	101	101	104	113	124	134
101	101	101	101	101	(101)	101	104	113	124	134
100	100	100	100	100	97	99	98	103	113	124
100	100	100	100	100	97	99	98	103	113	124
97	99	99	98	93	95	94	98	106	120	135
97	99	99	98	93	95	94	98	106	120	135
100	100	97	98	94	93	95	94	95	96	97

Figure 34. VIS (top) and IR bottom) digital count value matrices for surface ship location 43.8N 143.1W (center of data matrix), 0000 GMT, 5 August 1976.

121	123	127	122	120	124	131	130	126	120	127
121	121	121	124	125	132	139	133	128	117	116
115	119	124	127	133	140	129	124	120	117	111
119	132	132	137	134	122	120	115	102	101	103
135	143	141	131	117	116	110	95	102	130	154
132	131	123	108	104	96	92	131	148	156	159
113	106	94	89	89	101	143	146	153	146	150
93	88	88	96	130	147	160	153	147	139	141
73	84	130	151	155	146	146	142	137	137	157
116	154	150	144	140	139	137	138	137	147	154
144	135	136	128	128	147	143	142	153	152	157

95	95	96	98	99	100	102	103	103	104	102
95	95	96	98	99	100	102	103	103	104	102
101	107	111	112	115	115	112	110	105	100	95
101	107	111	112	115	115	112	110	105	100	95
111	117	120	120	117	115	108	102	95	94	94
111	117	120	120	117	115	108	102	95	94	94
120	117	115	112	107	99	97	94	94	94	94
120	117	115	112	107	99	97	94	94	94	94
110	105	101	98	95	94	94	94	94	95	95
110	105	101	98	95	94	94	94	94	95	95
97	94	91	93	93	93	94	94	94	95	95

Figure 35. VIS (top) and IR (bottom) digital count value matrices for surface ship location 43.5N 153.9W (center of data matrix), 0000 GMT, 6 August 1976.

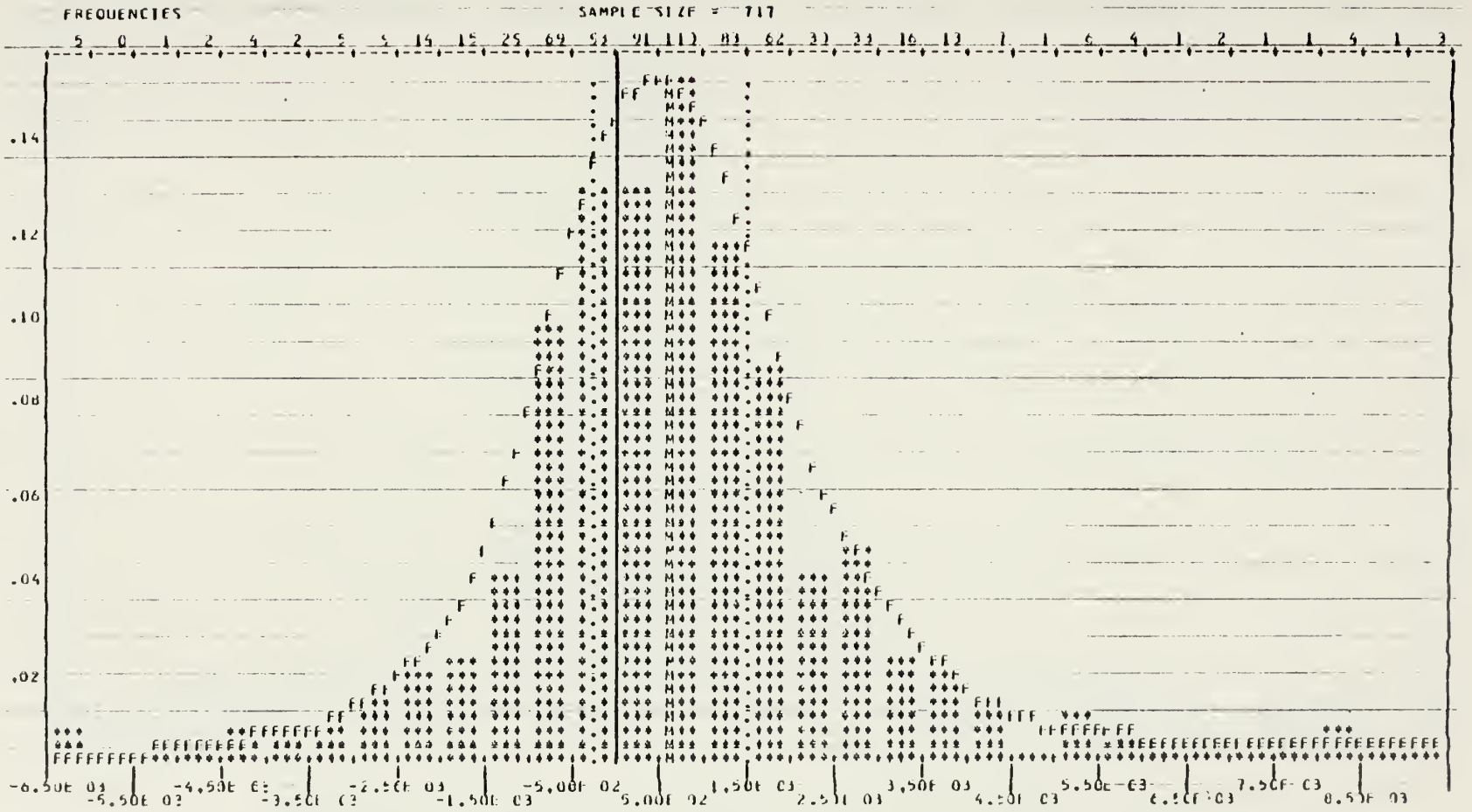

Figure 36. Frequency distribution of SMS-2 cloud base height (in meters) for all fog duration categories (see Tables II and III); 30-60N, eastern North Pacific Ocean, 5-9 August 1976; (1) frequencies and sample size along abscissa (top), (2) percentage frequencies along ordinate, (3) M = mean DCV, (4) F = empirical density function.

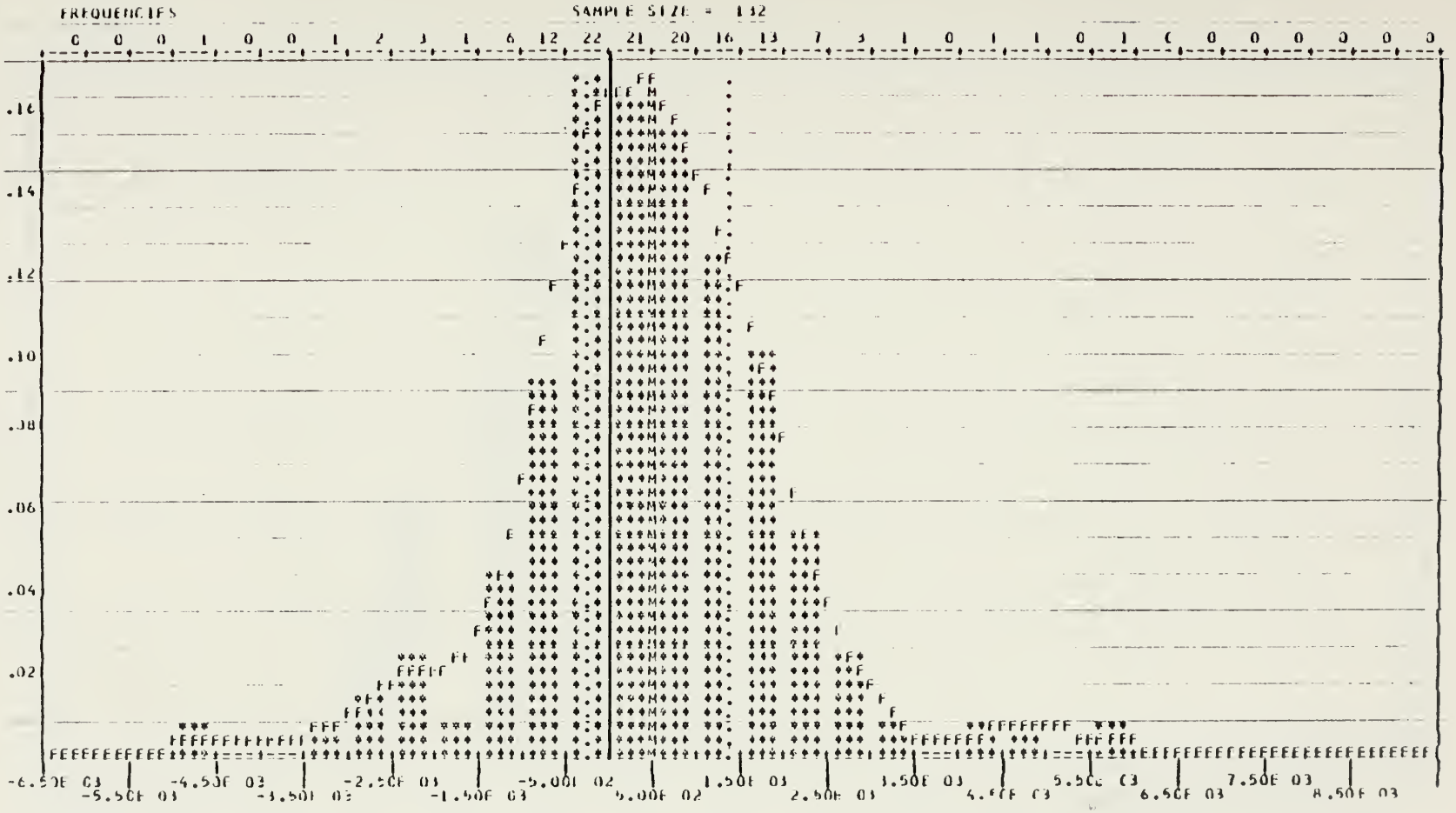

Figure 37. Frequency distribution of SMS-2 cloud base height (in meters) for fog duration category group 1 (see Tables II and III); 30-60N, eastern North Pacific Ocean, 5-9 August 1976; (1) frequencies and sample size along abscissa (top), (2) percentage frequencies along ordinate, (3) M = mean DCV, (4) F = empirical density function.

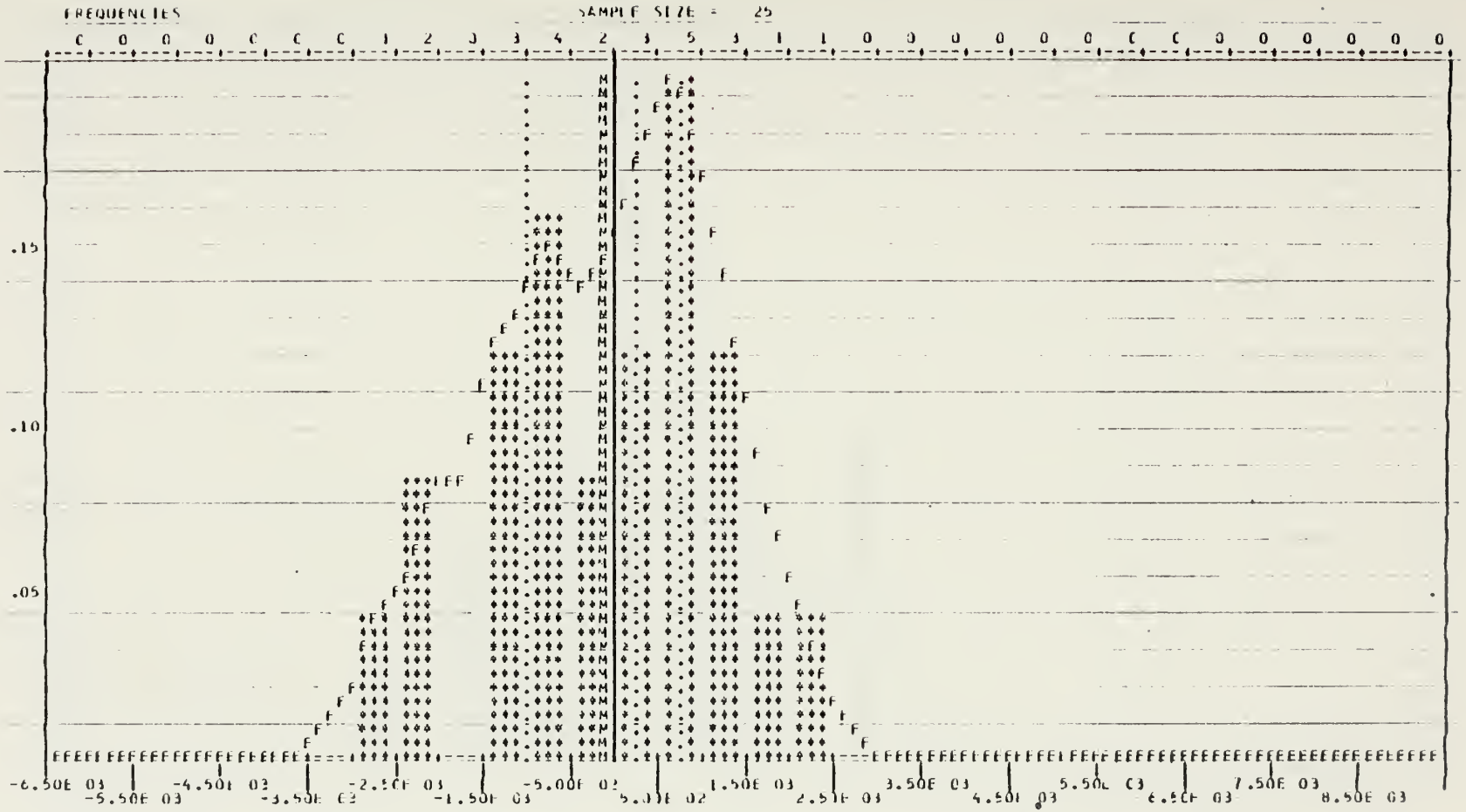

Figure 38. Frequency distribution of SMS-2 cloud base height (in meters) for fog duration category group 2 (see Tables II and III); 30-60N, eastern North Pacific Ocean, 5-9 August 1976; (1) frequencies and sample size along abscissa (top), (2) percentage frequencies along ordinate, (3) M = mean DCV, (4) F = empirical density function.

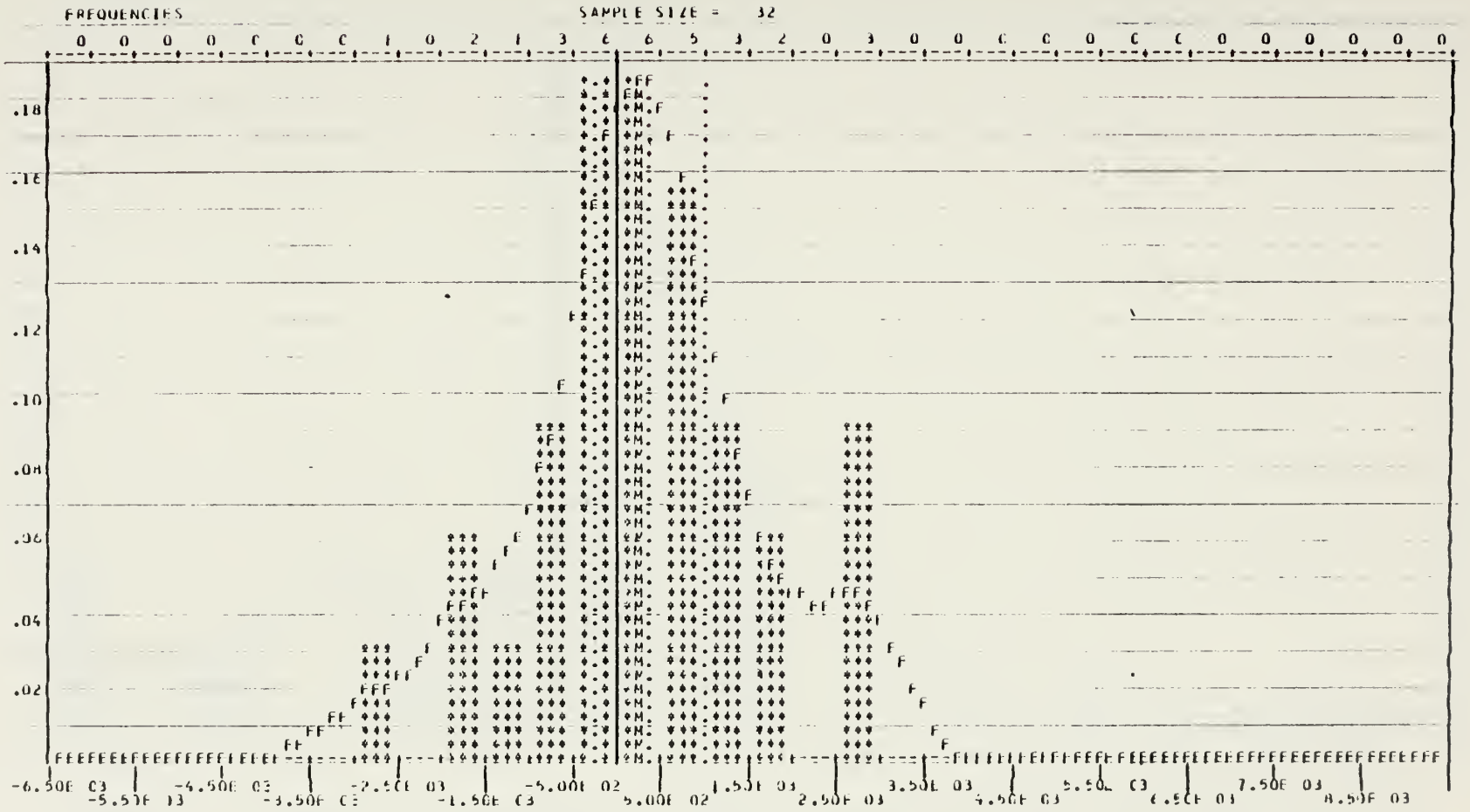

Figure 39. Frequency distribution of SMS-2 cloud base height (in meters) for fog duration category group 3 (see Tables II and III); 30-60N, eastern North Pacific Ocean, 5-9 August 1976; (1) frequencies and sample size along abscissa (top), (2) percentage frequencies along ordinate, (3) M = mean DCV, (4) F = empirical density function.

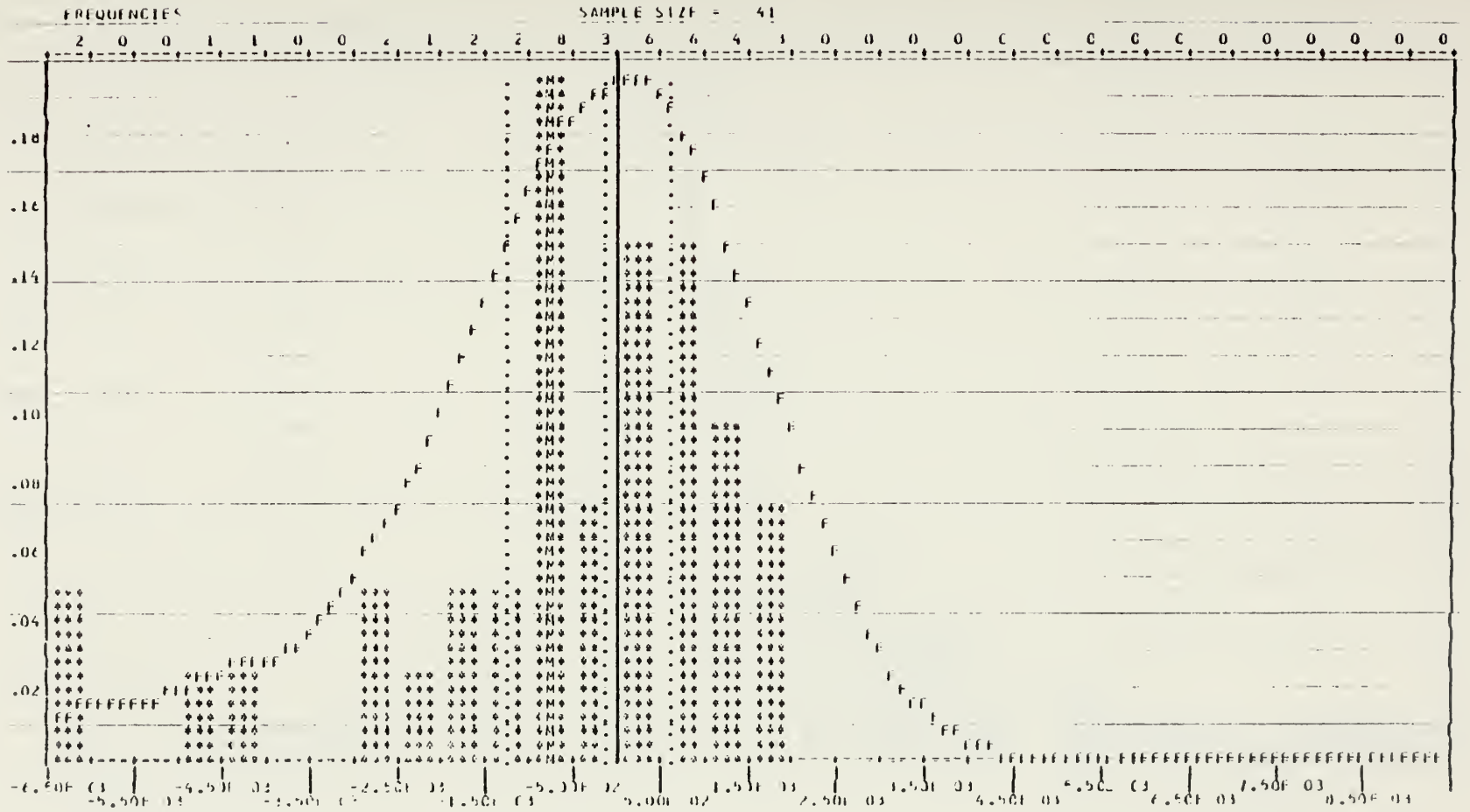

Figure 40. Frequency distribution of SMS-2 cloud base height (in meters) for fog duration category 175 (see Tables II and III); 30-60N, eastern North Pacific Ocean, 5-9 August 1976; (1) frequencies and sample size along abscissa (top), (2) percentage frequencies along ordinate, (3) M = mean DCV, (4) F = empirical density function.

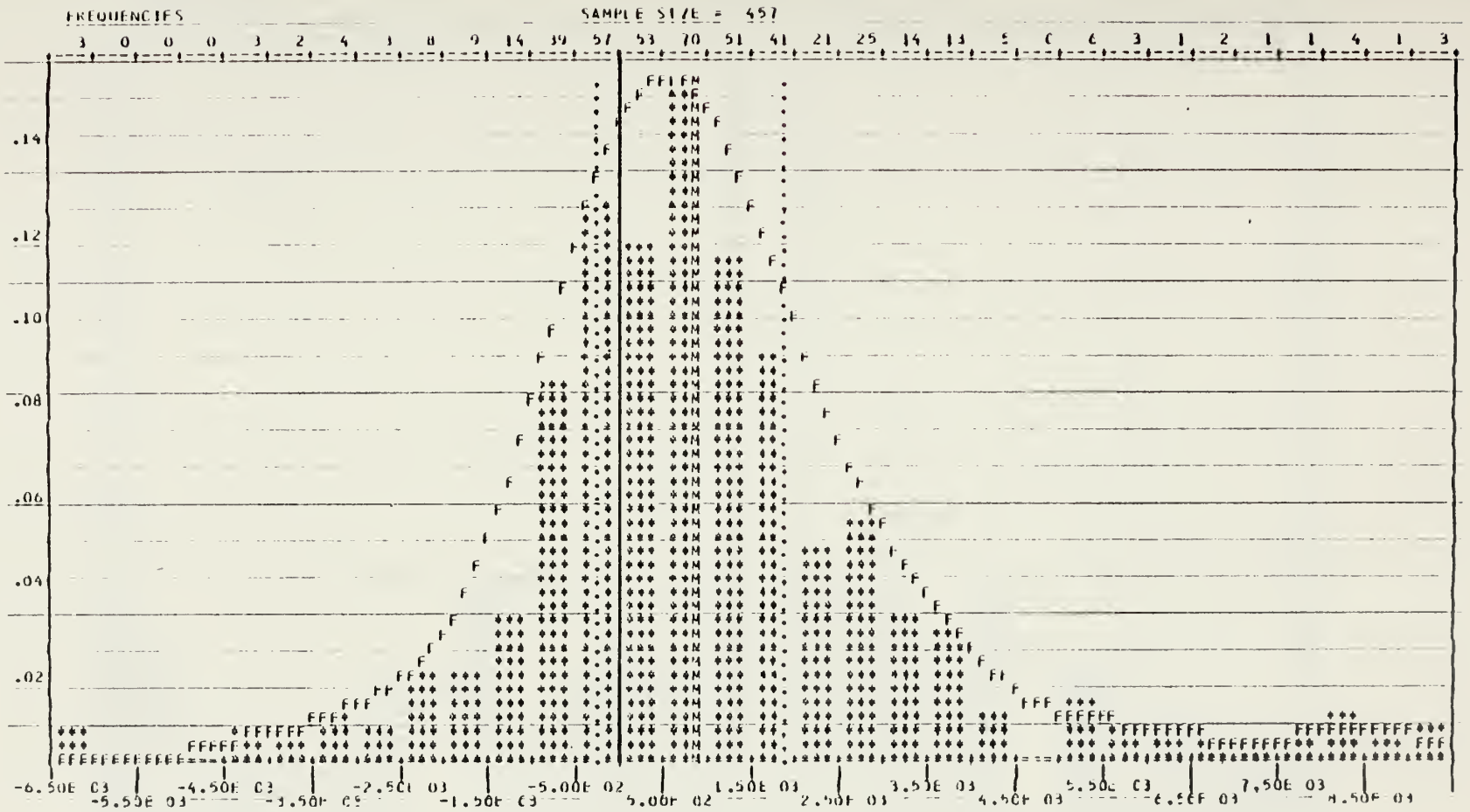

Figure 41. Frequency distribution of SMS-2 cloud base height (in meters) for fog duration category 180 (see Tables II and III); 30-60N, eastern North Pacific Ocean, 5-9 August 1976; (1) frequencies and sample size along abscissa (top), (2) percentage frequencies along ordinate, (3) M = mean DCV, (4) F = empirical density function.

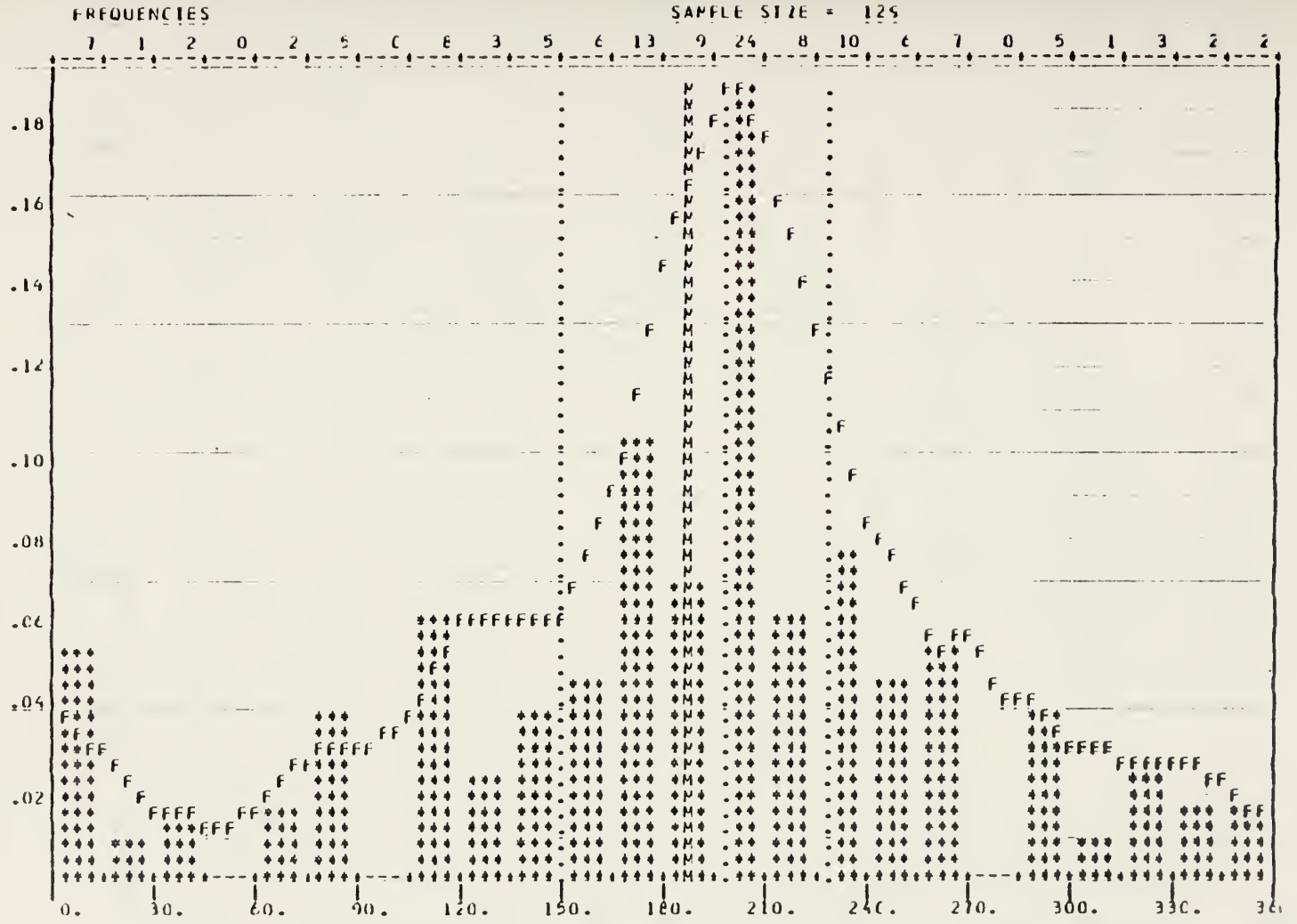

Figure 42. Frequency distribution of surface winds for synoptic ship reports; fog duration category group 1 (see Tables II and III); 30-60N, eastern North Pacific Ocean, 5-9 August 1976; (1) frequencies and sample size along abscissa (top), (2) percentage frequencies along ordinate, (3) M = mean DCV, (4) F = empirical density function.

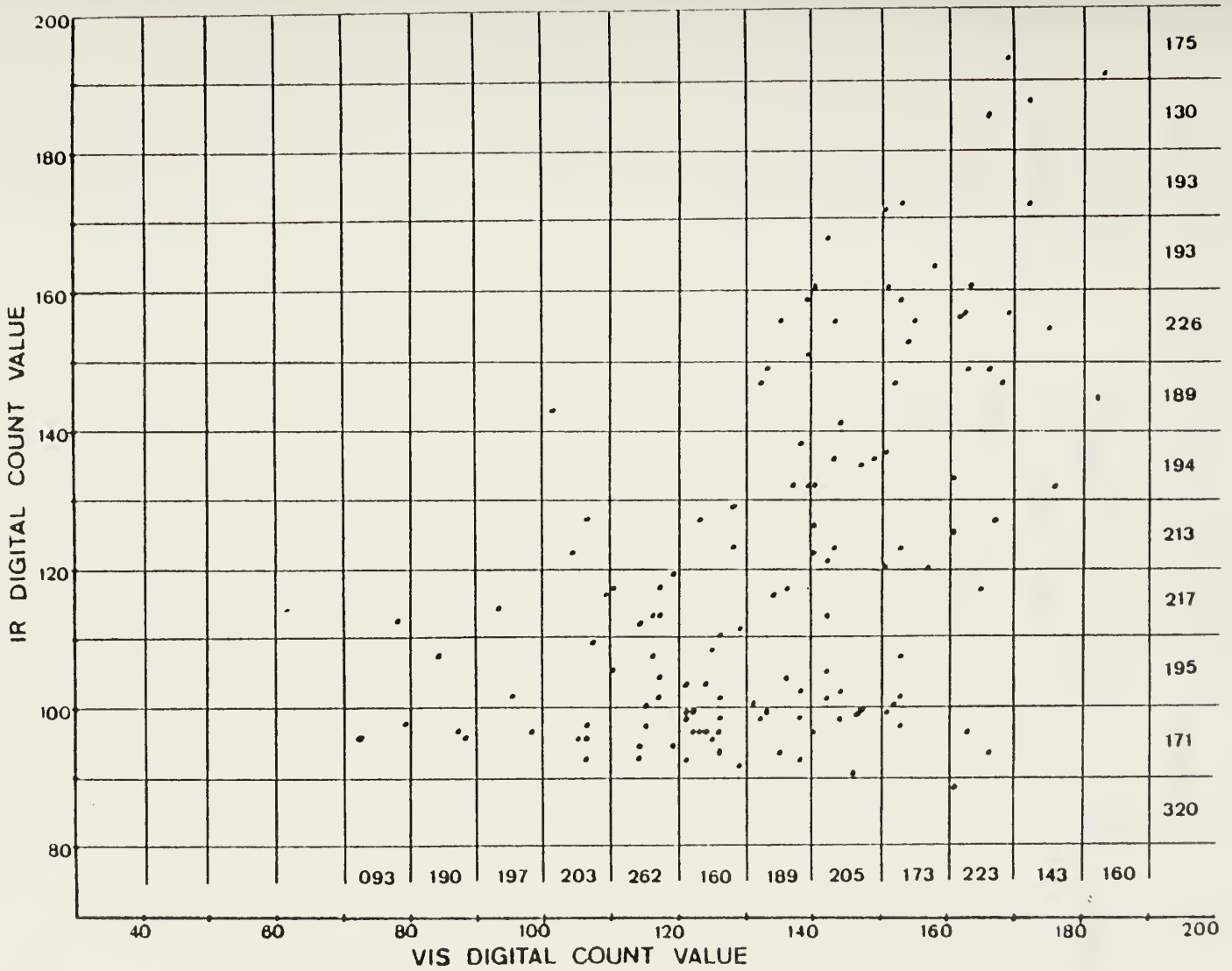

Figure 43. Mean surface wind directions averaged by column (along VIS axis) and row (along IR axis); fog duration category group 1 (see Tables II and III); 30-60N, eastern North Pacific Ocean, 5-9 August 1976.

TABLE I

DMSP data interval as a function of latitude

Latitude	I-J grid size (nmi)	Data interval (nmi)
Equator	110.4 by 110.4	1.73
30N	165.6 by 165.6	2.59
45N	188.5 by 188.5	2.95
60N	206 by 206	3.22

TABLE II. Marine-fog duration categories as dependent on the visibility-weather group elements of the primary synoptic report. Hours of fog assigned are derived from an analysis of summer-season North Pacific Ocean Weather Station (P,Q,S) weather log data (after Willms, 1975).

Fog Duration Categories	Coded Visibility	Coded Present Weather	Coded Past Weather	Hours of Fog Assigned
10	*	40-49	4	5.5
15	*	40-49	5	4.3
20	*	10	4	5.1
22	*	11,12	4	3.0
24	*	10	5	3.0
26	*	11,12	5	2.0
30	90-93	**	4	4.7
31	90-93	H	4	3.0
32	94	**	4	3.8
33	94	H	4	3.0
35	90-93	**	5	3.8
36	90-93	H	5	2.0
37	94	**	5	1.2
38	94	H	5	1.0
40	*	28	4	5.3
45	*	28	5,6	3.3
50	*	40-49	6	3.6
60	*	10	6	2.6
65	*	11,12	6	1.0
70	90-93	**	6	2.9
71	90-93	H	6	1.0
72	94	**	6	1.0
73	94	H	6	1.0
80	*	40-49	2	4.0
90	*	10	2	3.5
95	*	11,12	2	1.0
100	90-93	**	2	2.5
102	94	**	2	1.3
110	*	28	2	4.6
120	*	**	4	3.1
130	*	40-49	0,1,3,7-9	3.6
140	*	10	0,1,3,7-9	2.6
145	*	11,12	0,1,3,7-9	1.0
150	90-93	**	0,1,3,7-9	1.0
152	94	**	0,1,3,7-9	1.0
160	*	28	0,1,3,7-9	3.3
175	95-96	**	0-3,5-9	0.6
180	All reports not fitting above categories			

* Denotes any visibility allowed, i.e. 90-99

** Denotes any present weather code except 10,11,12,28,40-49 or heavy present weather codes

H Denotes heavy present weather codes only: 30-39, 62-65, 67, 69, 72-75, 81, 82, 84, 86, 88, 90-99

TABLE III. Fog duration category (FDC) groupings.

Group	Assumed Weather Condition	FDC's included
FDC Group 1 (FDC GR 1)	heavy fog likely at observation time	10,15,30,35,50, 70,80,100,130
FDC Group 2 (FDC GR 2)	light fog likely at observation time	20,24,32,37,60, 90,140
FDC Group 3 (FDC GR 3)	fog likely but not necessarily at observation time	22,26,40,73,110, 120
FDC 175	visibility qualifies for light fog, but fog not reported	175
FDC 180	no fog	180

TABLE IV. DMSP histogram statistics.

Histogram	Figure No.	DMSP Data	Range of Count Values (0-62 possible)	Total no. of reports
All FDC	9	VIS	26 - 60	69
All FDC	11	IR	19 - 46	116
FDC GR 1	10a	VIS	29 - 52	12
FDC GR 1	12a	IR	20 - 39	37
FDC GR 2, FDC GR 3, FDC 175	10b	VIS	28 - 55	12
FDC GR 2, FDC GR 3	12b	IR	19 - 38	14
FDC 175	12d	IR	20 - 38	11
FDC 180	10c	VIS	26 - 60	42
FDC 180	12c	IR	20 - 46	50

TABLE V. SMS-2 histogram statistics.

Histogram	Figure	Range of Count Values	Total no. of reports	Mean value
VIS All FDC	13	39 - 198	715	121.7
VIS FDC GR 1	14	74 - 184	131	135.6
VIS FDC GR 2	15	92 - 160	24	135.9
VIS FDC GR 3	16	62 - 184	32	134.2
VIS FDC 175	17	47 - 198	41	142.8
VIS FDC 180	18	39 - 185	457	114.0
IR All FDC	19	73 - 196	714	115.6
IR FDC GR 1	20	89 - 195	131	121.3
IR FDC GR 2	21	95 - 191	24	124.6
IR FDC GR 3	22	96 - 180	32	118.8
IR FDC 175	23	76 - 190	41	129.6
IR FDC 180	24	73 - 196	456	112.1

TABLE VI. SMS-2 VIS/IR count value range before/after removal of middle/high clouds.

FDC Group	No. of reports	No. of reports after apparent middle and high cloud cases removed	Digital count value range VIS before	VIS after	IR before	IR after
FDC GR 1	131	74	74-184	78-168	89-195	89-130
FDC GR 2	24	16	92-160	92-160	95-191	95-132
FDC GR 3	32	23	62-184	62-167	96-180	96-120
FDC 175	41	18	47-198	47-168	76-190	76-126

TABLE VII. SMS-2 cloud base height statistics.

Histogram	Figure	Mean height (m)	Total no. of reports
All FDC	36	651.5	717
FDC GR 1	37	462.9	132
FDC GR 2	38	-121.8	25
FDC GR 3	39	287.6	32
FDC 175	40	-842.6	41
FDC 180	41	915.2	457

LIST OF REFERENCES

Chatters, G. C. and Suomi, V. E., 1975: The Applications of MCIDAS. IEEE Transactions on Geoscience Electronics, GE-13, 137-146.

Hale, R. E. and Renard, R. J., 1975: Use of the NOAA-2 Digitized Satellite Data for Diagnosing Marine Fog in the North Pacific Ocean Area. NPS-51H175091, Naval Postgraduate School, Monterey, California, 92 pp.

Mosher, F. R., 1974: SMS Cloud Heights. Unpublished manuscript, Space Science and Engineering Center, University of Wisconsin, Madison, Wisconsin, 27 pp.

Renard, R. J., Englebretson, R. E. and Daughenbaugh, J. S., 1975: Climatological Marine Fog Frequencies Derived from a Synthesis of the Visibility-Weather Group Elements of the Transient-Ship Synoptic Reports. NPS-51Rd75031, Naval Postgraduate School, Monterey, California, 40 pp.

Smith, E. A., 1975: The MCIDAS System. IEEE Transactions on Geoscience Electronics, GE-13, 123-136.

U. S. Naval Weather Service Command, 1975: U. S. Naval Weather Service Numerical Environmental Products Manual, NAVAIR 50-1G-522, Department of the Navy, Washington, D. C.

Wallace, R. T. and Renard, R. J., 1975: The Use of Meteorological Satellites for Discerning Marine Fog. NPS-51Wa-75031, Naval Postgraduate School, Monterey, California, 59 pp.

Wheeler, S. E., 1974: Marine Fog Impact on Naval Operations. M. S. Thesis, Department of Oceanography, Naval Postgraduate School, Monterey, California, 118 pp.

Willms, G. R., 1-75: A Climatology of Marine-Fog Frequencies for the North Pacific Ocean Summer Fog Season. M. S. Thesis, Department of Meteorology, Naval Postgraduate School, Monterey, California, 59 pp.

INITIAL DISTRIBUTION LIST

		No. Copies
1.	Department of Oceanography, Code 68 Naval Postgraduate School Monterey, California 93940	3
2.	Oceanographer of the Navy Hoffman Building No. 2 200 Stovall Street Alexandria, Virginia 22332	1
3.	Office of Naval Research Code 480 Arlington, Virginia 22217	1
4.	Dr. Robert E. Stevenson Scientific Liaison Office, ONR Scripps Institution of Oceanography La Jolla, California 92037	1
5.	Library, Code 3330 Naval Oceanographic Office Washington, D. C. 20373	1
6.	SIO Library University of California, San Diego P. O. Box 2367 La Jolla, California 92037	1
7.	Department of Oceanography Library University of Washington Seattle, Washington 98105	1
8.	Department of Oceanography Library Oregon State University Corvallis, Oregon 97331	1
9.	Commanding Officer Fleet Numerical Weather Central Monterey, California 93940	1
10.	Commanding Officer Navy Environmental Prediction Research Facility Monterey, California 93940	1
11.	Defense Documentation Center Cameron Station Alexandria, Virginia 22314	2

12. Department of the Navy — 1
Commander Oceanographic System Pacific
Box 1390
FPO San Francisco 96610

13. Library, Code 0142 — 2
Naval Postgraduate School
Monterey, California 93940

14. National Center for Atmospheric Research — 1
Library Acquisitions
Boulder, Colorado 80301

15. Dr. James L. Kassner, Jr. — 1
Graduate Center for Cloud Physics Research
University of Missouri
Rolla, Missouri 65401

16. Director, Naval Oceanography and Meteorology — 1
National Space Technology Laboratories
Bay St. Louis, Mississippi 39520

17. Air Weather Service — 1
(AWVAS/TF)
Scott AFB, Illinois 62225

18. Department of Meteorology Code 63 — 1
Naval Postgraduate School
Monterey, California 93940

19. Dr. Robert J. Renard, Code 63Rd — 8
Department of Meteorology
Naval Postgraduate School
Monterey, California 93940

20. Dr. Gordon E. Schacher, Code 61Sq — 1
Department of Physics and Chemistry
Naval Postgraduate School
Monterey, California 93940

21. Dr. Glenn H. Jung, Code 68 — 1
Department of Oceanography
Naval Postgraduate School
Monterey, California 93940

22. Dr. Dale F. Leipper, Code 68 — 1
Department of Oceanography
Naval Postgraduate School
Monterey, California 93940

23. Mr. Edward Barker — 1
Navy Environmental Prediction Research
Facility
Monterey, California 93940

24. Dr. Pierre St. Amand 1
Earth and Planetary Sci. Div. Code 602
Department of the Navy
Naval Weapons Center
China Lake, California 93555

25. Mr. Murray H. Schefer 1
AIR-370C
Naval Air Systems Command
Washington, D. C. 20360

26. Dr. Lothar Ruhnke 1
Naval Research Laboratory
Code 8320
Washington, D. C. 20390

27. Dr. Patrick Squires 1
Desert Research Institute
University of Nevada
Reno, Nevada 89507

28. Dr. Thomas E. Hoffer 1
Desert Research Institute
University of Nevada
Reno, Nevada 89507

29. Mr. James Hughes 1
Office of Naval Research
Code 412
Arlington, Virginia 22217

30. Mr. Paul R. Lowe 1
Navy Environmental Prediction Research
Facility
Monterey, California 93940

31. Mr. Roland Pilie 1
Calspan Corporation
Buffalo, New York 14221

32. Dr. Dee F. Taylor 1
Naval Air Systems Command
AIR-540
Washington, D. C. 20360

33. Captain Robert L. Zralek 1
1400 Lakeshore Drive
Chicago 10, Illinois

34. Mr. Gene Mack 1
Calspan Corporation
Buffalo, New York 14221

35. LT. Carl B. Ihli, USN — 4
U. S. Fleet Weather Central, Guam
Box 12, COMNAVMARIANAS
FPO San Francisco 96630

36. LT. Ronald E. Hale — 1
484 Hale Street
Chula Vista, California 92010

37. Mr. Thomas O. Haig — 1
Space Science and Engineering Center
1225 West Dayton Street
University of Wisconsin
Madison, Wisconsin 53706

38. Mr. Gary C. Chatters — 1
Space Science and Engineering Center
1225 West Dayton Street
University of Wisconsin
Madison, Wisconsin 53706

39. Mr. Frederick R. Mosher — 1
Space Science and Engineering Center
1225 West Dayton Street
University of Wisconsin
Madison, Wisconsin 53706

40. Mr. J. T. Young — 1
Space Science and Engineering Center
1225 West Dayton Street
University of Wisconsin
Madison, Wisconsin 53706

Thesis
I185
c.1

169898

Ihli

The use of DMSP and SMS-2 digital satellite data for identifying marine fog in the eastern North Pacific Ocean area.